

**FIG 10** HCV infection downregulates membrane expression of ENT1-GFP. (A) Expression of the ENT1-GFP chimera clone in uninfected Huh-7.5 cells in a kinetic study over 4 days. (B) RBV treatment has no effect on membrane expression of the ENT1-GFP chimera in Huh-7.5 cells. (C) Membrane expression of ENT1-GFP was downregulated when cells were treated with the indicated concentrations of Torin 1. (D) HCV infection impairs membrane expression of ENT1-GFP at the indicated time points. (E) Confocal images showing that ENT1-GFP expression is downregulated in HCV core-expressing cells. DAPI, 4',6-diamidino-2-phenylindole. (F) Effect of clathrin heavy chain and ATG16L1 knockdown by siRNA on expression of ENT1. Huh-7.5 cells transfected with control (All-Star-negative) or CHC and ATG16L1 siRNAs for 24 h were analyzed by Western blotting. ENT1 levels were decreased after CHC knockdown in Huh-7.5 cells compared to ATG16L1 knockdown. (G) Knockdown of clathrin heavy chain by siRNA impairs ENT1-GFP membrane expression in Huh-7.5 cells. Knockdown of ATG16L1 did not affect membrane expression of ENT1-GFP in Huh-7.5 cells.

inhibitors BafA1, 3-MA, and HCQ prevent ENT1 degradation and significantly induce RBV-mediated HCV clearance. These results suggest that RBV, along with autophagy inhibitors, may be used to improve the efficacy of RBV antiviral activity against HCV. This knowledge from HCV studies can be extended to improve the efficacy of RBV against other RNA and DNA viruses. Combination therapy of autophagy inhibitors along with RBV should be explored to inhibit chronic HCV infection, and the strategy may be extended to include the inhibition of other viral infections, such as RSV and LASV infections.

An understanding of the molecular basis for how cellular autophagy impairs RBV antiviral efficacy can open novel approaches for improving HCV clearance by antiviral therapy. Induction of autophagy by nutrient deprivation or viral infection causes dramatic increases in autophagosome formation and cellular lysosomal degradation. Autophagosomes originate from the ER

membrane, Golgi apparatus, plasma membrane, recycling of endosomes, and mitochondria (36). Recently, it was shown that plasma membrane-derived clathrin-coated vesicles become ATG16L1 positive through interactions between ATG16L1 and the clathrin heavy chain (31). Clathrin-coated vesicles play an important role in modulating the expression of cell surface proteins and receptors. Persistent HCV replication in Huh-7.5 cells induces an autophagy response and downregulates the expression of the clathrin heavy chain. We have confirmed this by flow sorting, colocalization studies using confocal microscopy, and Western blot analysis. Using a number of approaches, including the use of an ENT1-GFP chimera clone, we showed in this study that silencing of clathrin expression also abolishes ENT1 expression on hepatocyte membranes and that ENT1-GFP is concentrated in the perinuclear area, suggesting that it may be in the ER. Our results support the hypothesis that clathrin-mediated recycling of ENT1

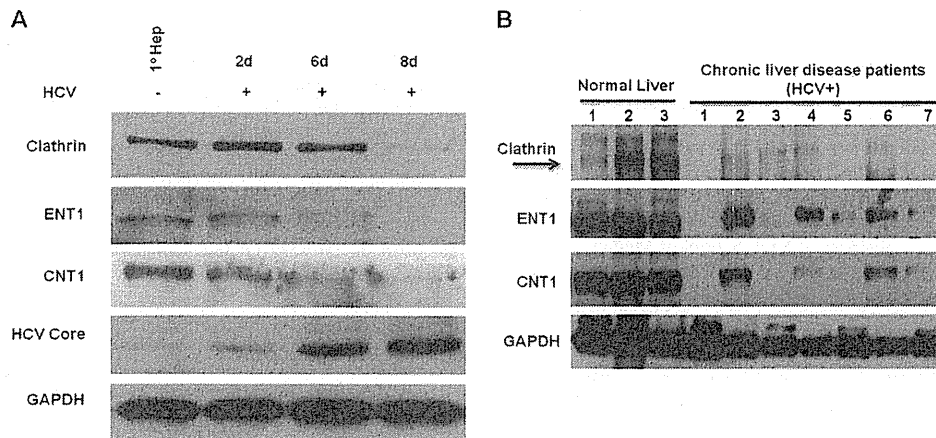


FIG 11 HCV infection reduces the expression of ENT1 and the clathrin heavy chain in infected primary human hepatocytes and HCV-infected human liver tissues. (A) Western blot analysis of clathrin, ENT1, CNT1, and core proteins in human hepatocytes infected with cell culture-grown HCV. (B) Western blot analysis for validation of clathrin, ENT1, and CNT1 in HCV-infected human liver biopsy specimens of seven patients and three normal uninfected liver samples.

is blocked by the HCV-induced autophagy response; HCV-induced autophagy response-mediated clathrin degradation prevents the recycling of ENT1, which forces it to the lysosome for degradation. These results indicate that clathrin degradation and ENT1 expression are regulated by the HCV-induced autophagy response.

Human ENTs, which occur as four isoforms (each with well-characterized structures and functions), play an important role in the transport of RBV molecules into hepatocytes (4). The ENT1 isoform, which is expressed primarily on the plasma membrane, is important in transporting nucleoside analogue drugs used in antiviral therapy. The ENT1 protein is translated and folded in the ER and is transported via the Golgi apparatus to the plasma membrane (23). In the plasma membrane, ENT1 is internalized by

clathrin-dependent endocytosis and recycled following clathrin-mediated internalization. The cell surface expression of ENT1 is hampered if the protein is not properly recycled to the plasma membrane, and defects in the recycling of ENT1 may lead to its degradation in lysosomal vesicles. Our study shows that clathrin-mediated endocytosis is selectively impaired in cells that are persistently infected with HCV. The level of clathrin is significantly decreased after HCV infection or autophagy induction. The HCV-induced autophagy response causes a defect in clathrin-mediated endocytosis, which is responsible for impaired RBV antiviral activity. Clathrin-mediated endocytosis is generally impaired in HCV-infected cells and underlies the impaired antiviral action of RBV via a blockade of ENT1 recycling. Endocytosis serves as an interface between the hepatocyte and its external environment

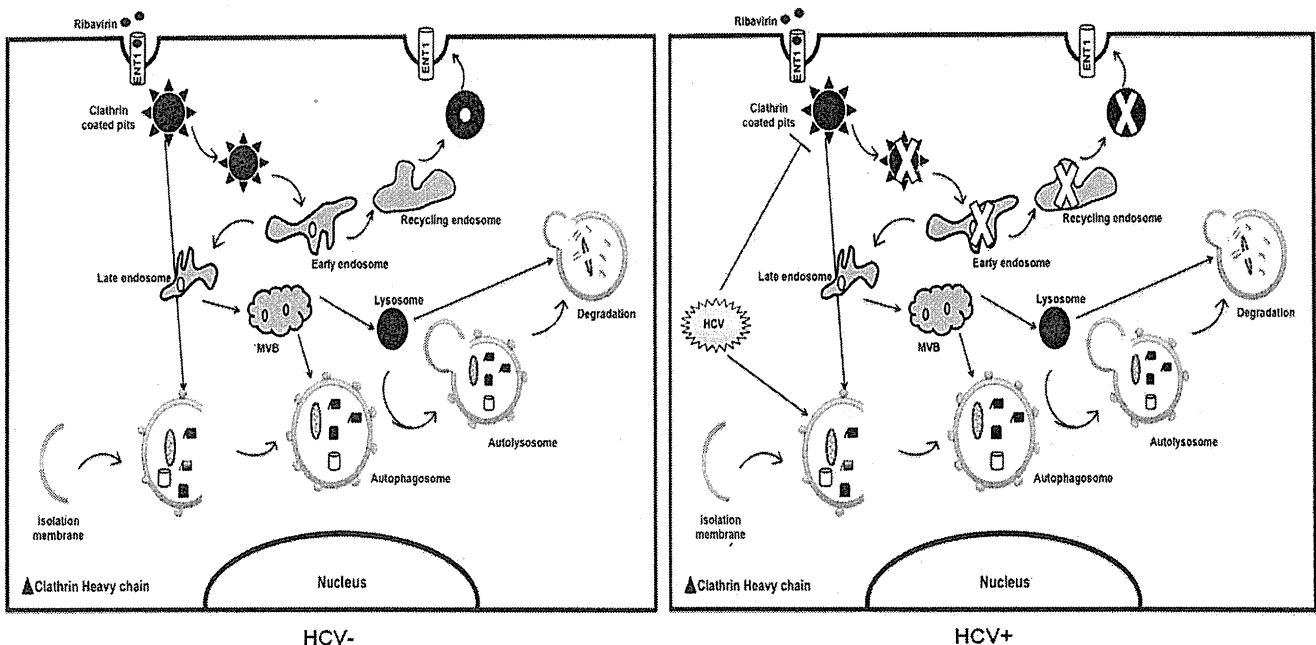


FIG 12 Diagram summarizing the proposed mechanism for impaired RBV antiviral activity against HCV in cell culture. MVB, multivesicular bodies.

and is important for the stable expression of a number of cell surface receptors and for intracellular signal transduction. The significance of HCV autophagy-mediated impairment of clathrin-mediated endocytosis requires further investigation to establish its clinical relevance in the pathogenesis of chronic HCV infection in humans.

## ACKNOWLEDGMENTS

We thank Charles M. Rice for providing Huh-7.5 cells and Shuanghu Liu and Curt H. Hagedorn, University of Utah School of Medicine, for providing the JFH- $\Delta$ V3-Rluc plasmid. We acknowledge Krzysztof Moroz for taking pictures of immunostaining slides. We acknowledge Asim Abdel-Mageed, Manish Ranjan, and Amanda Struckhoff for taking pictures of immunofluorescence slides.

This work was supported by NIH grants CA127481, CA089121, and AI103106 and by bridge funding received from the Tulane University Health Sciences Center.

## REFERENCES

- Mohd Hanafiah K, Groeger J, Flaxman AD, Wiersma ST. 2013. Global epidemiology of hepatitis C virus infection: new estimates of age-specific antibody to HCV seroprevalence. *Hepatology* 57:1333–1342. <http://dx.doi.org/10.1002/hep.26141>.
- Shiffman ML. 2014. Hepatitis C therapy in the direct acting antiviral era. *Curr Opin Gastroenterol* 30:217–222. <http://dx.doi.org/10.1097/MOG.000000000000062>.
- Casey LC, Lee WM. 2013. Hepatitis C virus therapy update 2013. *Curr Opin Gastroenterol* 29:243–249. <http://dx.doi.org/10.1097/MOG.0b013e32835ff972>.
- Clark V, Nelson DR. 2012. The role of ribavirin in direct acting antiviral drug regimens for chronic hepatitis C. *Liver Int* 32:103–107. <http://dx.doi.org/10.1111/j.1478-3231.2011.02711.x>.
- Casey J, Morris K, Narayana M, Nakagaki M, Kennedy GA. 2013. Oral ribavirin for the treatment of respiratory syncytial virus and parainfluenza 3 virus infections post-allogeneic hematopoietic stem cell transplantation. *Bone Marrow Transplant* 48:1558–1561. <http://dx.doi.org/10.1038/bmt.2013.112>.
- McCormick JB, King IJ, Webb PA, Scribner CL, Craven RB, Johnson KM, Elliott LH, Belmont-Williams R. 1986. Lassa fever. Effective therapy with ribavirin. *N Engl J Med* 314:20–26.
- Dixit NM, Perelson AS. 2006. The metabolism, pharmacokinetics and mechanisms of antiviral activity of ribavirin against hepatitis C virus. *Cell Mol Life Sci* 63:832–842. <http://dx.doi.org/10.1007/s00018-005-5455-y>.
- Lanford RE, Chavez D, Guerra B, Lau JY, Hong Z, Brasky KM, Beames B. 2001. Ribavirin induces error-prone replication of GB virus B in primary tamarin hepatocytes. *J Virol* 75:8074–8081. <http://dx.doi.org/10.1128/JVI.75.17.8074-8081.2001>.
- Paeshuyse J, Dallmeier K, Neyts J. 2011. Ribavirin for the treatment of chronic hepatitis C virus infection: a review of the proposed mechanism of action. *Curr Opin Virol* 1:590–598. <http://dx.doi.org/10.1016/j.coviro.2011.10.030>.
- Kong W, Engel K, Wang J. 2004. Mammalian nucleoside transporters. *Curr Drug Metab* 5:63–84. <http://dx.doi.org/10.2174/1389200043489162>.
- Feld JJ, Hoofnagle JH. 2005. Mechanism of action of interferon and ribavirin in treatment of hepatitis C. *Nature* 436:967–972. <http://dx.doi.org/10.1038/nature04082>.
- Panigrahi R, Hazari S, Chandra S, Chandra PK, Datta S, Kurt R, Cameron CE, Huang Z, Zhang H, Garry RF, Balart LA, Dash S. 2013. Interferon and ribavirin combination treatment synergistically inhibit HCV internal ribosome entry site mediated translation at the level of poly-ribosome formation. *PLoS One* 8:e72791. <http://dx.doi.org/10.1371/journal.pone.0072791>.
- Pfeiffer JK, Kirkegaard K. 2005. Ribavirin resistance in hepatitis C virus replicon-containing cell lines conferred by changes in the cell line or mutations in the replicon RNA. *J Virol* 79:2346–2355. <http://dx.doi.org/10.1128/JVI.79.4.2346-2355.2005>.
- Hmwe SS, Aizaki H, Date T, Murakami K, Ishii K, Miyamura T, Koike K, Wakita T, Suzuki T. 2010. Identification of hepatitis C virus genotype 2a replicon variants with reduced susceptibility to ribavirin. *Antiviral Res* 85:520–524. <http://dx.doi.org/10.1016/j.antiviral.2009.12.008>.
- Ibarra KD, Jain MK, Pfeiffer JK. 2011. Host-based ribavirin resistance influences hepatitis C virus replication and treatment response. *J Virol* 85:7273–7273. <http://dx.doi.org/10.1128/JVI.00629-11>.
- Ibarra KD, Pfeiffer JK. 2009. Reduced ribavirin antiviral efficacy via nucleoside transporter-mediated drug resistance. *J Virol* 83:4538–4547. <http://dx.doi.org/10.1128/JVI.02280-08>.
- Iikura M, Furihata T, Mizuguchi M, Nagai M, Ikeda M, Kato N, Tsubota A, Chiba K. 2012. ENT1, a ribavirin transporter, plays a pivotal role in antiviral efficacy of ribavirin in a hepatitis C virus replication cell system. *Antimicrob Agents Chemother* 56:1407–1413. <http://dx.doi.org/10.1128/AAC.05762-11>.
- Mori K, Hiraoka O, Ikeda M, Ariumi Y, Horamoto A, Wataya Y, Kato N. 2013. Adenosine kinase is a key determinant for anti-HCV activity of ribavirin. *Hepatology* 58:1236–1244. <http://dx.doi.org/10.1002/hep.26421>.
- Shah NR, Sunderland A, Grdzlishvili VZ. 2010. Cell type mediated resistance of vesicular stomatitis virus and Sendai virus to ribavirin. *PLoS One* 5:e11265. <http://dx.doi.org/10.1371/journal.pone.0011265>.
- Chandra PK, Bao L, Song K, Aboulnasr FM, Baker DP, Shores N, Wimley WC, Liu S, Hagedorn CH, Fuchs SY, Wu T, Balart LA, Dash S. 2014. HCV infection selectively impairs type I but not type III IFN signaling. *Am J Pathol* 184:214–229. <http://dx.doi.org/10.1016/j.ajpath.2013.10.005>.
- Datta S, Hazari S, Chandra PK, Samara M, Poat B, Gunduz F, Wimley WC, Hauser H, Koster M, Lamaze C, Balart LA, Garry RF, Dash S. 2011. Mechanisms of HCV's resistance to IFN-alpha in cell culture involve expression of functional IFN-alpha receptor 1. *Virology* 423:351–351. <http://dx.doi.org/10.1016/j.viro.2011.03.008>.
- Liu S, Nelson CA, Xiao L, Lu L, Seth PP, Davis DR, Hagedorn CH. 2011. Measuring antiviral activity of benzimidazole molecules that alters IRES RNA structure with an infectious hepatitis C virus chimera expressing Renilla luciferase. *Antiviral Res* 89:54–63. <http://dx.doi.org/10.1016/j.antiviral.2010.11.004>.
- Nivillac NM, Bacani J, Coe IR. 2011. The life cycle of human equilibrative nucleoside transporter 1: from ER export to degradation. *Exp Cell Res* 317:1567–1579. <http://dx.doi.org/10.1016/j.yexcr.2011.03.008>.
- Skrypek N, Duchene B, Hebbar M, Leteurtre E, van Seuning I, Jonckheere N. 2013. The MUC4 mucin mediates gemcitabine resistance of human pancreatic cancer cells via the concentrative nucleoside transporter family. *Oncogene* 32:1714–1723. <http://dx.doi.org/10.1038/ncr.2012.179>.
- Dreux M, Chisari FV. 2011. Impact of the autophagy machinery on hepatitis C virus infection. *Viruses* 3:1342–1352. <http://dx.doi.org/10.3390/v3081342>.
- Klionsky DJ, Codogno P, Cuervo AM, Deretic V, Elazar Z, Fueyo-Margareto J, Gewirtz DA, Kroemer G, Levine B, Mizushima N, Rubinsztein DC, Thumm M, Tooze SA. 2010. A comprehensive glossary of autophagy-related molecules and processes. *Autophagy* 6:438–448. <http://dx.doi.org/10.4161/autophagy.6.4.12244>.
- Tanida I, Ueno T, Kominami E. 2008. LC3 and autophagy. *Methods Mol Biol* 445:77–88. [http://dx.doi.org/10.1007/978-1-59745-157-4\\_4](http://dx.doi.org/10.1007/978-1-59745-157-4_4).
- Bao L, Chandra PK, Moroz K, Zhang X, Thung SN, Wu T, Dash S. 2014. Impaired autophagy response in human hepatocellular carcinoma. *Exp Mol Pathol* 96:149–154. <http://dx.doi.org/10.1016/j.yexmp.2013.12.002>.
- Yang YP, Hu LF, Zheng HF, Mao CJ, Hu WD, Xiong KP, Wang F, Liu CF. 2013. Application and interpretation of current autophagy inhibitors and activators. *Acta Pharmacol Sin* 34:625–635. <http://dx.doi.org/10.1038/aps.2013.5>.
- Rong Y, Liu M, Ma L, Du W, Zhang H, Tian Y, Cao Z, Li Y, Ren H, Zhang C, Li L, Chen S, Xi J, Yu L. 2012. Clathrin and phosphatidylinositol-4,5-bisphosphate regulate autophagic lysosome reformation. *Nat Cell Biol* 14:924–934. <http://dx.doi.org/10.1038/ncb2557>.
- Ravikumar B, Moreau K, Jahreiss L, Puri C, Rubinsztein DC. 2010. Plasma membrane contributes to the formation of pre-autophagosomal structures. *Nat Cell Biol* 12:747–757. <http://dx.doi.org/10.1038/ncb2078>.
- Chandra PK, Gunduz F, Hazari S, Ramazan K, Panigrahi R, Poat B, Bruce D, Cohen AJ, Behorquez HE, Carmody I, Loss G, Balart LA, Wu T, Dash S. 2014. Impaired expression of type I and type II interferon receptors in HCV-associated chronic liver disease and liver cirrhosis. *PLoS One* 9:e108616. <http://dx.doi.org/10.1371/journal.pone.0108616>.
- Hoofnagle JH, Lau D, Conjeevaram H, Kleiner D, Di Bisceglie AM.

1996. Prolonged therapy of chronic hepatitis C with ribavirin. *J Viral Hepat* 3:247–252. <http://dx.doi.org/10.1111/j.1365-2893.1996.tb00050.x>.
34. Reddy KR, Shiffman ML, Rodriguez-Torres M, Cheinquer H, Abdurakhmanov D, Bakulin I, Morozov V, Silva GF, Geyvandova N, Stanciu C, Rabbia M, McKenna M, Thommes JA, Harrison SA, PROGRESS Study Investigators. 2010. Induction pegylated interferon alfa-2a and high dose ribavirin do not increase SVR in healthy patients with genotype 1a and high viral loads. *Gastroenterology* 139:1972–1983. <http://dx.doi.org/10.1053/j.gastro.2010.08.051>.
35. Rautou PE, Cazals-Hatem D, Feldmann G, Mansouri A, Grodet A, Barge S, Martinot-Peignoux M, Duces A, Bièche I, Lebre C, Bedossa P, Paradis V, Marcellin P, Valla D, Asselah T, Moreau R. 2011. Changes in autophagic response in patients with chronic hepatitis C virus infection. *Am J Pathol* 178:2708–2715. <http://dx.doi.org/10.1016/j.ajpath.2011.02.021>.
36. Lamb CA, Yoshimori T, Tooze SA. 2013. The autophagosome; origins unknown, biogenesis complex. *Nat Rev Mol Cell Biol* 14:759–774. <http://dx.doi.org/10.1038/nrm3696>.



# Involvement of MAP3K8 and miR-17-5p in Poor Virologic Response to Interferon-Based Combination Therapy for Chronic Hepatitis C

Akihito Tsubota<sup>1,2\*</sup>, Kaoru Mogushi<sup>3</sup>, Hideki Aizaki<sup>4</sup>, Ken Miyaguchi<sup>3</sup>, Keisuke Nagatsuma<sup>1,2</sup>, Hiroshi Matsudaira<sup>1,2</sup>, Tatsuya Kushida<sup>5</sup>, Tomomi Furihata<sup>6</sup>, Hiroshi Tanaka<sup>3</sup>, Tomokazu Matsuura<sup>7</sup>

**1** Institute of Clinical Medicine and Research (ICMR), Jikei University School of Medicine, Kashiwa, Chiba, Japan, **2** Division of Gastroenterology and Hepatology, Kashiwa Hospital, The Jikei University School of Medicine, Kashiwa, Chiba, Japan, **3** Department of Bioinformatics, Medical Research Institute, Tokyo Medical and Dental University, Bunkyo-ku, Tokyo, Japan, **4** Department of Virology II, National Institute of Infectious Diseases, Shinjuku-ku, Tokyo, Japan, **5** National Bioscience Database Center, Japan Science and Technology Agency, Chiyoda-ku, Tokyo, Japan, **6** Laboratory of Pharmacology and Toxicology, Graduate School of Pharmaceutical Science, Chiba University, Chiba, Japan, **7** Department of Laboratory Medicine, Jikei University School of Medicine, Minato-ku, Tokyo, Japan

## Abstract

Despite advances in chronic hepatitis C treatment, a proportion of patients respond poorly to treatment. This study aimed to explore hepatic mRNA and microRNA signatures involved in hepatitis C treatment resistance. Global hepatic mRNA and microRNA expression profiles were compared using microarray data between treatment responses. Quantitative real-time polymerase chain reaction validated the gene signatures from 130 patients who were infected with hepatitis C virus genotype 1b and treated with pegylated interferon-alpha and ribavirin combination therapy. The correlation between mRNA and microRNA was evaluated using *in silico* analysis and *in vitro* siRNA and microRNA inhibition/overexpression experiments. Multivariate regression analysis identified that the independent variables IL28B SNP rs8099917, hsa-miR-122-5p, hsa-miR-17-5p, and MAP3K8 were significantly associated with a poor virologic response. MAP3K8 and miR-17-5p expression were inversely correlated with treatment response. Furthermore, miR-17-5p repressed HCV production by targeting MAP3K8. Collectively, the data suggest that several molecules and the inverse correlation between mRNA and microRNA contributed to a host genetic refractory hepatitis C treatment response.

**Citation:** Tsubota A, Mogushi K, Aizaki H, Miyaguchi K, Nagatsuma K, et al. (2014) Involvement of MAP3K8 and miR-17-5p in Poor Virologic Response to Interferon-Based Combination Therapy for Chronic Hepatitis C. PLoS ONE 9(5): e97078. doi:10.1371/journal.pone.0097078

**Editor:** Wenyu Lin, Harvard Medical School, United States of America

**Received:** December 6, 2013; **Accepted:** April 14, 2014; **Published:** May 12, 2014

**Copyright:** © 2014 Tsubota et al. This is an open-access article distributed under the terms of the Creative Commons Attribution License, which permits unrestricted use, distribution, and reproduction in any medium, provided the original author and source are credited.

**Funding:** This work was supported in part by Grants-in-Aid from the Ministry of Health, Labour and Welfare (Japan), the Ministry of Education, Culture, Sports, Science and Technology (Japan), and Clinical Research Funds from ICMR, the Jikei University School of Medicine. The funders had no role in study design, data collection and analysis, decision to publish, or preparation of the manuscript.

**Competing Interests:** The authors have declared that no competing interests exist.

\* E-mail: atsubo@jikei.ac.jp

## Introduction

Chronic hepatitis C (CH-C) caused by hepatitis C virus (HCV) infection is a major chronic liver disease worldwide, and it often develops into cirrhosis and hepatocellular carcinoma. Pegylated interferon alpha (peg-IFN $\alpha$ ) and ribavirin (RBV) combination therapy is widely used to treat CH-C [1]. However, treatment fails in approximately 50% patients with HCV genotype 1. Of note, approximately 20–30% patients show null or partial response to the treatment. The introduction of nonstructural 3/4A protease inhibitors has improved the outcome for genotype 1 CH-C patients [1]. However, new antiviral agents increase the frequency and severity of adverse effects, are costly, have complex treatment regimens, and often result in viral resistance. Importantly, the outcomes of triple combination therapy are extremely poor in patients who showed null and partial response to previous peg-IFN $\alpha$ /RBV, compared to treatment-naïve patients and relapsers [1–3]. Furthermore, over 50% of null and partial responders, among all patients with a similar virologic response or viral kinetics, relapse after treatment cessation [2,3]. Collectively, these studies suggest a role of host genetics in treatment resistance.

Microarray applications in clinical medicine identified that numerous mRNAs and microRNAs (miRNAs) regulate complex processes involved in disease development. For example, hepatic mRNA expression of IFN-stimulated genes (ISGs, such as ISG15, OAS, IFI, IP10, and viperin) and IFN-related pathway genes (MX and USP18) correlate with responses to peg-IFN $\alpha$ /RBV combination therapy for CH-C [4–7]. However, few studies have examined global miRNAs alone [8]. Furthermore, mRNA and miRNA gene signatures and their interactions in treatment response have not been reported. miRNAs are evolutionarily conserved, small non-coding RNAs [9,10]. A single miRNA can regulate the expression of multiple target mRNAs and their encoded proteins by imperfect base pairing and subsequent mRNA cleavage/translational repression. Conversely, the expression of a single mRNA is often regulated by several miRNAs. As regulators of promotion or suppression of gene expression, miRNAs are involved in diverse biological and physiological processes, including cell cycle, proliferation, differentiation, and apoptosis. In addition to targeting endogenous mRNAs, miRNAs regulate the life cycle of viruses such as the Epstein-Barr virus,

HCV, and other oncogenic viruses by interacting with viral transcripts [11,12].

We investigated the differential expression profiles of mRNAs and miRNAs isolated from the liver tissues of untreated patients with HCV genotype 1b using microarray analysis. Expression profiles and their interactions were analyzed to identify the molecular signatures associated with treatment resistance.

## Materials and Methods

### Patient population, treatment, and liver tissue samples

During 2010 and 2011, 130 patients infected with HCV genotype 1b were treated weekly with 1.5 µg/kg of peg-IFN $\alpha$ -2b (MSD, Tokyo) and daily with 600–1000 mg RBV (MSD) [2,3] for 48 weeks at Jikei University Kashiwa-affiliated hospitals. Patients with undetectable serum HCV RNA at week 12 or later were recommended to extend the treatment to 72 weeks. All study participants provided informed written consent and materials for genetic testing and met the following criteria: (1) CH-C diagnosis confirmed by laboratory tests, virology, and histology; (2) genotype 1b confirmed by polymerase chain reaction (PCR)-based method; (3) absence of malignancy, liver failure, or other form of chronic liver disease; and (4) no concurrent treatment with any other antiviral or immunomodulatory agent. Liver specimens were obtained percutaneously before treatment, formalin-fixed, and paraffin-embedded for histological assessment [13]. A tissue section was stored in RNAlater solution (Life Technologies, Carlsbad, CA). Total RNA containing mRNA and miRNA was isolated using the mirVana miRNA isolation kit (Life Technologies).

Sustained virological response (SVR) was defined as an undetectable serum HCV RNA level at 24 weeks after treatment completion. A null response was defined as a viral decline of  $< 2 \log_{10}$  IU/mL from baseline at treatment week 12 and detectable HCV RNA during treatment. A partial response was defined as a viral decline of  $> 2 \log_{10}$  IU/mL from baseline at week 12, with no achievement of an undetectable HCV RNA level. Relapse was defined as an undetectable serum HCV RNA level at the end of treatment and viremia reappearance on follow-up examination [1]. Viral loads and the presence or absence of serum HCV RNA were evaluated using a qualitative PCR assay (Amplicor HCV version 2.0; Roche Diagnostics, Tokyo).

This study conformed to the provisions of the Declaration of Helsinki and Good Clinical Practice guidelines and was approved by the Jikei University Ethics Committee for Human Genome/Gene Analysis Research (No.21-093\_5671).

### mRNA microarray

Global mRNA expression analysis was performed using total RNA isolated from each sample [sustained virological responders (SVRs),  $n = 5$ ; relapsers,  $n = 3$ ; null responders,  $n = 4$ ] and the GeneChip Human Genome U133 Plus 2.0 Array (Affymetrix, Santa Clara, CA). Datasets were normalized by the robust multi-array analysis, using R 2.12.1 statistical software and the BioConductor package.

### miRNA microarray

Global miRNA expression analysis was performed using total RNA isolated from the same samples used for mRNA expression analysis and the miRCURY LNA microRNA Array series (Exiqon, Vedbaek, Denmark). Total RNA was labeled with Hy3 and hybridized to slides that contained capture probes targeting all human miRNAs registered in the miRBASE 14.0. miRNA

microarray datasets were normalized by quantile normalization using R statistical software.

### Differential gene expression according to treatment response

The limma package from BioConductor software (under R statistical software) was used to calculate moderated t-statistics (based on the empirical Bayes approach) to identify mRNA or miRNA differentially expressed between the SVR/relapser group and null/partial responder group. Because of multiple hypothesis testing,  $p$  values were adjusted by the Benjamini-Hochberg false discovery rate (FDR) method.

### Hierarchical cluster analysis

Up- and down-regulated probe sets were analyzed by hierarchical clustering using R statistical software. Pearson's correlation coefficients were used to calculate a matrix similarity score among the probe sets. The complete linkage method was used for agglomeration. Heat maps were generated from significant differentially expressed probe sets.

### Quantitative real-time PCR for mRNA

To validate microarray results and to confirm the observed differences in the mRNA expression levels in a quantitative manner, each sample was subjected to reverse transcription (RT)-PCR and quantitative real-time RT-PCR (qPCR) in triplicate. After cDNA synthesis, target genes were amplified in PCR mixtures that contained TaqMan Universal PCR Master Mix (Life Technologies) and TaqMan probes designed with the Universal Probe Library Assay Design Center (<http://www.roche-applied-science.com/sis/rtqcr/upl/adc.jsp>). Target gene expression levels in each sample were normalized to the expression of the housekeeping gene of 18S rRNA and the corresponding gene of one null responder.

### Quantitative real-time PCR for miRNA

cDNA was synthesized from aliquots of the isolated total RNA using the TaqMan MicroRNA Reverse Transcription kit (Life Technologies) including RT primers designed with miRNA-specific stem-loop structures according to manufacturer's protocol. miRNA expression levels were quantified with the TaqMan MicroRNA assay (Life Technologies) in triplicate. Target gene expression levels were normalized in each sample to the expression of the endogenous gene RNU48 and the corresponding gene of one null responder.

### miRNA target prediction

Up- and down-regulated miRNAs with a fold change of  $> 1.2$  and  $p < 0.005$  (FDR  $< 0.15$ ) between two groups (SVRs/relapsers vs null responders) in the microarray analysis were subjected to the *in silico* prediction of mRNA targets for miRNA using MicroCosm Targets, miRanda, PicTar, PITA, and TargetScan algorithms. Predicted mRNA targets were analyzed further if they met the following criteria: (1) fold change of  $> 1.5$  and  $p < 0.003$  (FDR  $< 0.35$ ) in mRNA microarray results; (2) inverse correlation (negative correlation coefficient) between miRNA and mRNA in mRNA and miRNA microarray results; and (3) qPCR-validated microarray results. Kyoto Encyclopedia of Genes and Genomes (KEGG) Pathways, Agilent Literature Search 3.0.3 beta, and Cytoscape 3.0.2 were used to identify the significance of candidates in gene regulatory networks.

## Cell culture

The human hepatoma cell line Huh7.5.1 (a gift from Professor Francis Chisari, Scripps Research Institute, La Jolla, CA) was maintained in Dulbecco's modified Eagle's medium containing 10% fetal bovine serum [14]. Cell culture-produced HCV (HCVcc) were harvested from JFH1-transfected Huh7.5.1 as previously described [15].

## Plasmids and siRNAs

The siRNAs targeting MAP3K8 were siRNA1, 5'-uucguccuuuauaucuugugt-3'; siRNA2, 5'-uguugcuagguuuauauactt-3'; siRNA3, 5'-aucuuguccaaguuauacctt-3'; and scrambled negative control siRNA to siRNA1 (Sigma-Aldrich, St. Louis, MO). The expression and inhibitor plasmids of hsa-miR-17-5p and control plasmids were purchased from GeneCopeia (Rockville, MD).

## HCV core antigen measurements and cell viability

The HCV core antigen concentrations in filtered culture medium and cell lysates of infected cells were measured with the Lumipulse Ortho HCV antigen kit (Ortho Clinical Diagnostics, Tokyo). Cell viability was analyzed using the CellTiter-Glo Luminescent Cell Viability Assay (Promega, Madison, WI).

## Transfection

Cells were seeded into a 24-well plate and transfected with siRNAs and plasmids using Lipofectamine RNAiMAX (Invitrogen, San Diego, CA) and TransIT-LT1 (Mirus, Madison, WI), respectively.

## Luciferase reporter assay

The MAP3K8 3'UTR segment containing the putative miR-17-5p target sites was subcloned into the pGL3 reporter plasmid (Promega). A mutant construct was also generated by PCR-based mutagenesis using mutagenic primers. The luciferase reporter and hsa-miR-17-5p expressing or mock plasmids were co-transfected with the *Renilla* luciferase transfection control plasmid. Luciferase reporter activity was measured 48 hours after transfection with the Dual-Luciferase Reporter Assay System (Promega).

## Western blot

Liver samples were sonicated in lysis buffer. Lysate aliquots were separated by SDS-polyacrylamide gel electrophoresis and transferred onto a nitrocellulose membrane. Membranes were incubated with primary antibodies against MAP3K8 (ab70853, Abcam, San Diego, CA) and  $\beta$ -actin (EP1123Y, Abcam). Membranes were incubated with horseradish peroxidase-conjugated secondary antibodies. Immunoreactivity was detected with reagents (GE Healthcare Life Sciences, Piscataway, NJ). Images were scanned and band intensities quantified with Image J.

## IL28B and ITPA single nucleotide polymorphism (SNP) genotyping

Genomic DNA was extracted from whole blood using the MagNA Pure LC and the DNA Isolation Kit (Roche Diagnostics). The IL28B rs8099917 and rs12979860 [16,17] and ITPA exon 2 rs1127354 [18] genetic polymorphisms were genotyped by real-time detection PCR with the TaqMan SNP Genotyping Assays.

## Statistical analysis for factors associated with null/partial response

The chi-square, Fisher's exact, Student's *t*, and the Mann-Whitney two-tailed tests were used to compare frequencies in categorical data or differences in continuous data between two

groups. Significant independent factors associated with null/partial responses were identified with multiple logistic regression analysis using the SPSS statistical package for Windows, version 17.0 (IBM SPSS, Chicago, IL). A *p* value of <0.05 was considered statistically significant.

## Results

### Patient profiles and treatment response

Among the 130 patients, 62 (48%) achieved SVR, 36 (28%) relapsed, and six (5%) and 26 (20%) showed partial and null response, respectively. Patients were divided into an SVR/relapser group and a null/partial responder group. Table S1 compares the baseline characteristics of the two groups. Patients with elevated serum gamma glutamyl transpeptidase and decreased albumin concentrations were more likely to experience a null/partial response. The IL28B rs8099917 TG and rs12979860 CT variants were more likely to be null/partial responders compared with TT and CC genotypes, respectively.

### mRNAs associated with treatment response

mRNA microarray data were deposited into the NCBI Gene Expression Omnibus (GEO) (<http://www.ncbi.nlm.nih.gov/geo/>), accession number GSE42697. The cut-off criteria for fold change >1.5 and *p*<0.003 identified 39 up-regulated and 17 down-regulated annotated probe sets in null responders (Data S1). The up-regulated genes were associated with transcription, translation, cell cycle, phosphorylation, signal transduction, immune response, RNA splicing/mRNA processing, and viral reproduction. The down-regulated genes were associated with xenobiotic/small molecule/lipid metabolic and oxidation-reduction processes. Hierarchical clustering of mRNAs and samples showed that samples from SVRs and relapsers clustered to form a group different from the null responders (Fig. S1). To validate the microarray results, qPCR was performed for all significant differentially expressed genes. The expression levels of MAP3K8 (mitogen-activated protein kinase kinase kinase 8, *p* =  $5.24 \times 10^{-7}$ ), TMEM178 (transmembrane protein 178, *p* =  $7.31 \times 10^{-6}$ ), PSME4 (proteasome activator subunit 4, also known as *P4200*, *p* =  $2.43 \times 10^{-4}$ ), and EIF3B (eukaryotic translation initiation factor-3B, *p* =  $3.16 \times 10^{-6}$ ; Fig. 1) were significantly increased in null/partial responders compared with those in SVRs/relapsers. TMEM178 is a multi-pass membrane protein and PSME4 is a nuclear protein that activates the proteasome and is important for oxidative-stress adaptation. EIF3B is involved in protein translation/synthesis and interacts with the HCV IRES and the 40S ribosomal subunit.

### miRNAs associated with treatment response

miRNA microarray data were deposited into the NCBI GEO, accession number GSE45179. The cut-off criteria for fold change >1.2 and *p*<0.005 identified 111 down-regulated and 76 up-regulated miRNAs in null responders (Data S2). Hierarchical two-dimensional clustering showed that distinct patient groups clustered into two distinct groups (Fig. S2). Bioinformatic analysis predicted target genes of the differentially expressed miRNAs. The hypothetical target genes should be MAP3K8, TMEM178, PSME4, and EIF3B. Furthermore, these miRNAs and mRNAs must have an inverse correlation between mRNA and miRNA microarray data. The microRNAs that satisfied the requirements were as follows: hsa-let-7g\* and hsa-miR-17-5p, -20b, -297, -374b, -494, -602, -668, and -1297 for MAP3K8; hsa-miR-106b\* and -122-5p for TMEM178; and hsa-miR-492 and -675-5p for PSME4. No corresponding miRNA was identified for EIF3B.

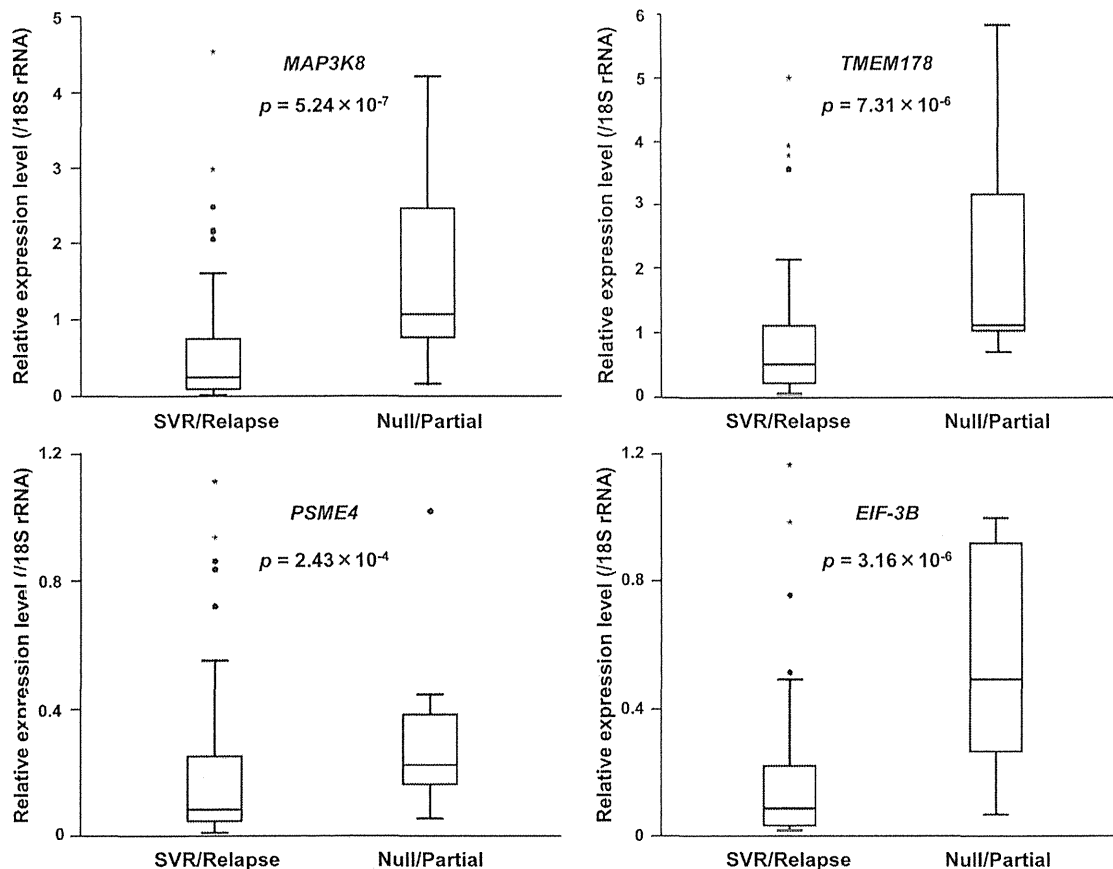


**Figure 1. Validation of differentially expressed mRNAs by qPCR analysis.** The expression levels of four mRNAs were significantly higher in null/partial responders than in SVRs/relapsers. Assays for each sample were performed in triplicate. All *p*-values were calculated using the Mann-Whitney test.

doi:10.1371/journal.pone.0097078.g001

Stem-loop-based qPCR was performed to confirm the reliability of the miRNA microarray results and the inverse correlation between miRNA and mRNA. The expression levels of hsa-miR-122-5p ( $p = 2.75 \times 10^{-8}$ ), hsa-miR-675-5p ( $p = 1.00 \times 10^{-5}$ ), and hsa-miR-17-5p ( $p = 1.73 \times 10^{-8}$ ) were significantly lower in null/partial responders than in SVRs/relapsers (Fig. 2).

#### Independent variables associated with treatment response

Multiple logistic regression analysis of variables that were significant in univariate analysis identified that rs8099917 [ $p = 3.67 \times 10^{-3}$ , odds ratio (OR) = 7.51, 95% confidence interval (CI) = 2.14–29.27], hsa-miR-122-5p ( $p = 5.60 \times 10^{-4}$ , OR = 0.11, 95% CI = 0.03–0.38), hsa-miR-17-5p ( $p = 2.02 \times 10^{-4}$ , OR = 0.56, 95% CI = 0.41–0.76), and MAP3K8 ( $p = 8.58 \times 10^{-3}$ , OR = 2.86, 95% CI = 1.31–6.25) were significantly associated with null/partial response. Importantly, *in silico* analysis and microarray data suggested that increased miR-17-5p could cause MAP3K8 reduction. In fact, an inverse correlation was observed between MAP3K8 mRNA and miR-17-5p ( $r = -0.592$ ,  $p = 4.31 \times 10^{-3}$ ). MAP3K8 is closely linked to genes associated with cell proliferation, inflammation, and apoptosis (Fig. S3) and is associated with the miR-17 cluster family (Fig. S4).

#### MAP3K8 contributes to HCV production

siRNA transfection in HCVcc-infected cells was performed to assess the influence of MAP3K8 mRNA and protein on HCV production (Fig. 3A). miR-17-5p levels were significantly increased (Fig. 3B) while supernatant HCV core antigen levels were significantly decreased following transfection of the siRNAs (Fig. 3C). However, the HCV core antigen levels in cell lysates were not changed (Fig. 3C). Taken together, these findings suggested that MAP3K8 repressed miR-17-5p and contributed to the production (e.g. release and assembly) of HCV. *In vivo*, MAP3K8 protein expression levels were significantly increased in null/partial responders compared with those in SVRs/relapsers ( $p = 2.43 \times 10^{-5}$ ).

#### Hsa-miR-17-5p regulates HCV production by targeting MAP3K8

Changes in MAP3K8 and HCV core antigen levels were evaluated by hsa-miR-17-5p inhibition and overexpression in HCVcc-infected cells. miR-17-5p inhibition increased MAP3K8 mRNA and protein levels (Fig. 4A and 4B, left). In contrast, miR-17-5p overexpression decreased MAP3K8 mRNA and protein levels (Fig. 4A and 4B, right). Interestingly, miR-17-5p inhibition increased, whereas miR-17-5p overexpression decreased HCV core antigen levels in both supernatants and cell lysates (Fig. 4C).



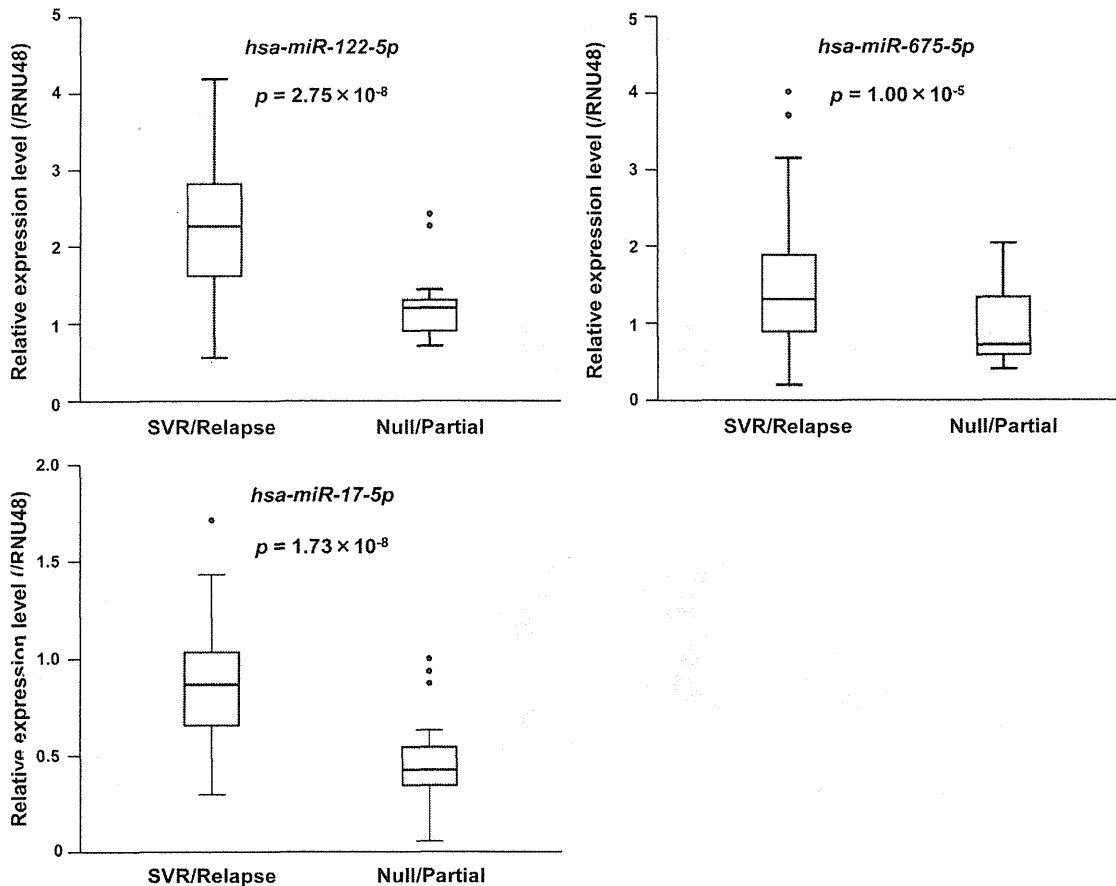


**Figure 2. Validation of differentially expressed miRNAs by qPCR analysis.** The expression levels of three miRNAs were significantly higher in null/partial responders than in SVRs/relapsers. Assays for each sample were performed in triplicate. All  $p$ -values were calculated using the Mann-Whitney test.

doi:10.1371/journal.pone.0097078.g002

Taken together, these results suggested that miR-17-5p regulated the production of HCV by targeting MAP3K8 mRNA. Luciferase reporter assays showed that miR-17-5p overexpression decreased the luciferase activity of the wild-type MAP3K8 3'UTR reporter construct, whereas co-transfection with the mutant MAP3K8 3'UTR construct or mock had no effect (Fig. 5), suggesting that miR-17-5p targeted the MAP3K8 3'UTR and antagonized MAP3K8 protein expression.

## Discussion

This study showed close linkage between mRNA and miRNA signatures in CH-C treatment outcomes using global expression profiling analyses. To confirm the findings, this cohort was randomly divided into derivation and confirmatory groups. The derivation group results were similar to those described above and reproducible in the confirmatory group (data not shown). Subsequently, we attempted to compare our findings with registered patient data obtained from independent cohorts comprising either Asian or non-Asian subjects. However, comparisons were not possible because most mRNA or miRNA microarray studies had a small sample size, limited information, unregistered data, and/or findings that were not validated in an independent cohort [4–7,11,19–21]. To our knowledge, our study

was the first to investigate the correlation between mRNA and miRNA in treatment response using global gene expression analysis and *in vitro* experiments. Such gene signature identification can improve the accuracy of treatment outcome predictions, independent of known strong predictors.

Pretreatment hepatic ISG levels are higher in non-SVRs/non-relapsers than in SVRs/relapsers [4–7]. The poor ISG response of non-SVRs with further exogenous IFN may contribute to treatment failure [5,6]. Because patient groups with different response categories differ in their innate IFN response to HCV infection; poor responders may have adopted a different equilibrium in their innate immune response to HCV [4,6]. As per multivariate regression analysis, however, IL28B SNPs may diminish the significance of hepatic ISGs as treatment predictors because hepatic ISG expression is associated with IL28B SNPs [7,19]. Conversely, hepatic ISGs were reported to be stronger predictors compared with IL28B SNPs [20]. Although our gene set enrichment analysis (data not shown) also showed that hepatic ISG expression levels were generally higher in null/partial responders than in SVRs/relapsers, the differences were not large enough to be ranked in a higher order and/or to reach statistical significance in expression profiling and validation analyses (Data S3). These variations among studies may be caused by different and heterogeneous patient characteristics, including HCV geno-

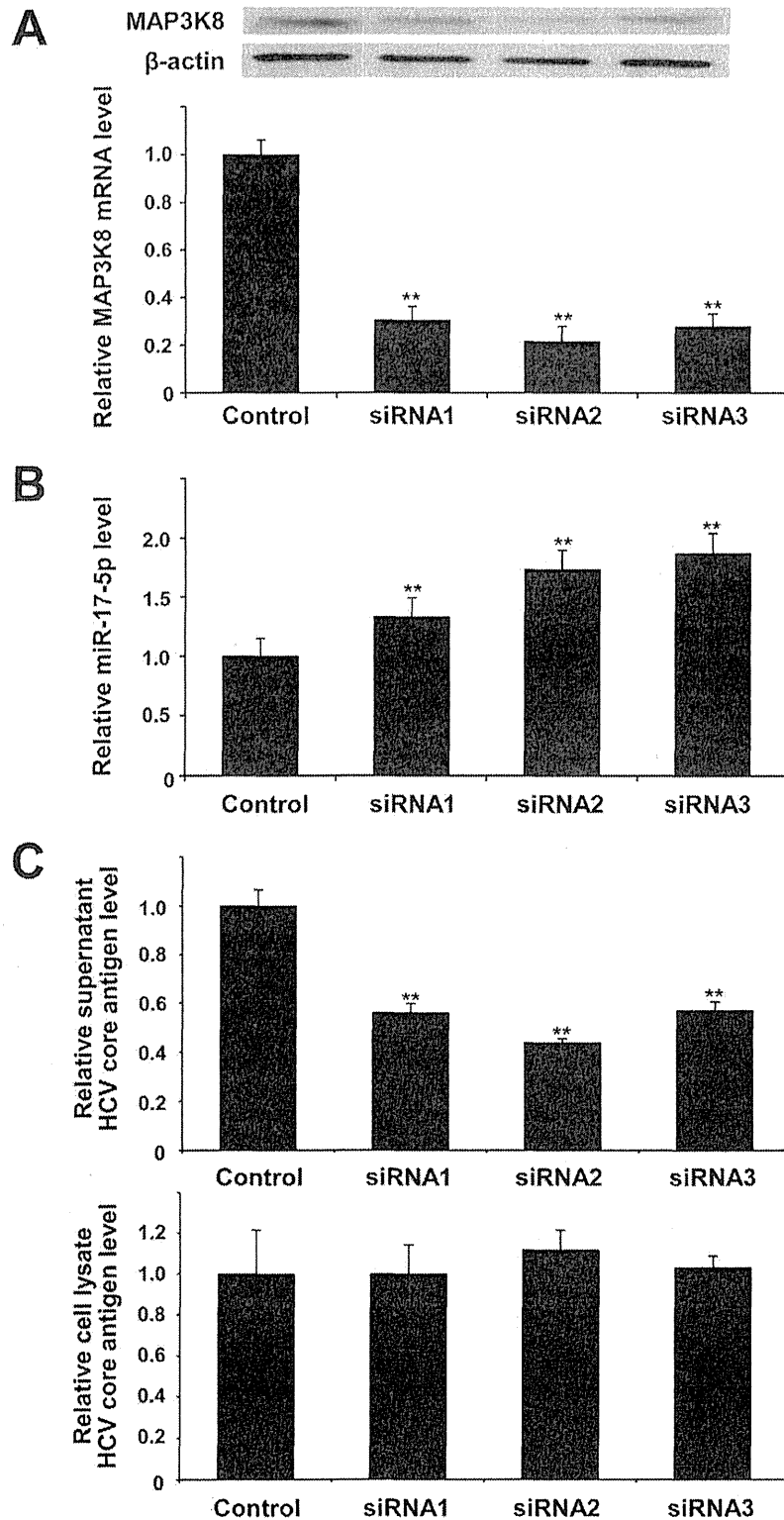


**Figure 3. Transfection of Huh7.5.1 cells with siRNAs against MAP3K8.** (A) Transfection of Huh7.5.1 cells with siRNAs against MAP3K8 significantly decreased intracellular MAP3K8 mRNA levels, (B) increased intracellular hsa-miR-17-5p levels, and (C) decreased HCV core antigen levels in the supernatant, and had no effect on those in cell lysate. Bars indicate the means of three independent experiments and the error bars indicate standard deviations. All *p*-values were calculated using two-tailed Student's *t*-test. \*\**p*<0.001 compared with controls. doi:10.1371/journal.pone.0097078.g003

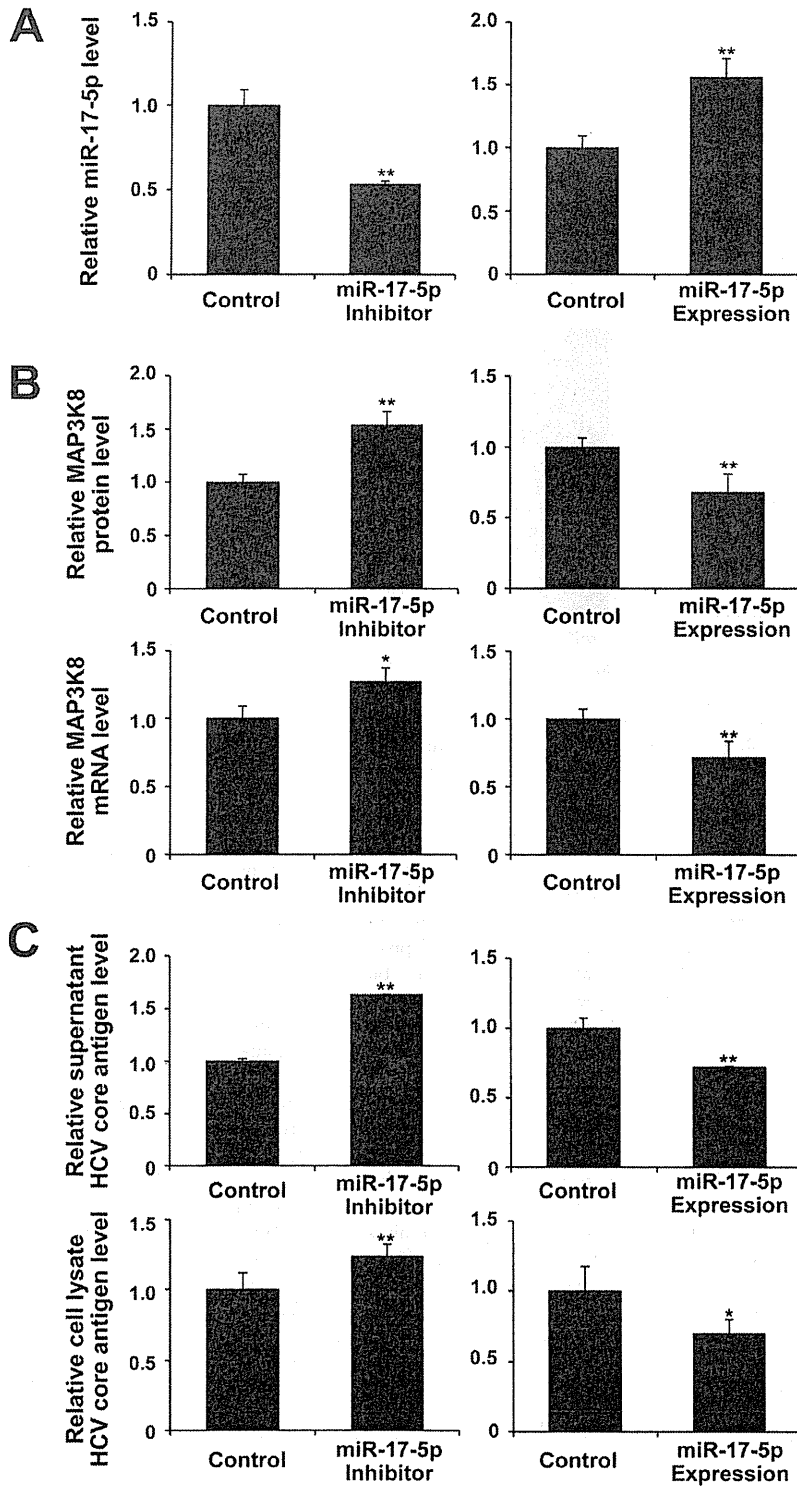


**Figure 4. Expression and inhibition of hsa-miR-17-5p in Huh7.5.1 cells.** (A) Functional suppression (left) and overexpression (right) plasmids of miR-17-5p. (B) Inhibition of miR-17-5p increased (left), whereas overexpression of miR-17-5p decreased MAP3K8 mRNA and protein expression levels (right). (C) HCV core antigen levels increased following miR-17-5p inhibition (left) and decreased by miR-17-5p overexpression (right) in both supernatant and cell lysate. Bars indicate the means of three independent experiments and the error bars indicate standard deviations. \* $p < 0.01$  and \*\* $p < 0.001$  compared with controls. doi:10.1371/journal.pone.0097078.g004

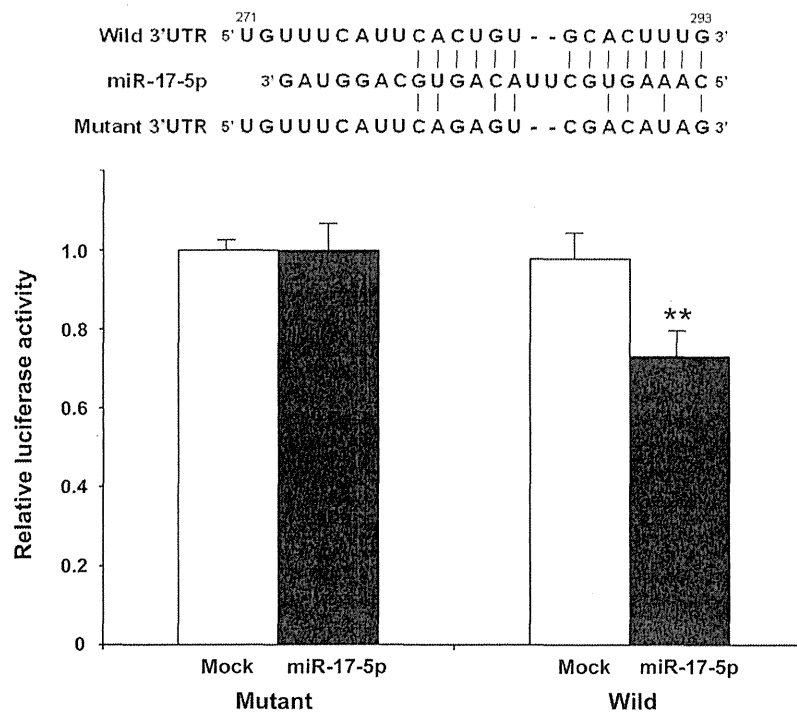


**Figure 5. Luciferase reporter assay.** miR-17-5p inhibited the luciferase activity of the wild-type MAP3K8 3'UTR construct (right), whereas no decrease in activity was observed in cells co-transfected with the mutant MAP3K8 3'UTR construct (left) or mock plus wild-type or mutant construct (right and left, respectively). Bars indicate the means of three independent experiments, and the error bars indicate standard deviations.  $**p < 0.001$  compared with controls.

doi:10.1371/journal.pone.0097078.g005

type, patient race, treatment response definitions, study endpoints, and treatment regimens. This study analyzed patients with a homogeneous race and genotype (1b) who adhered to combination therapy and treatment for a specified duration.

MAP3K8, also known as cancer Osaka thyroid (cot) [22] or tumor progression locus 2 (tpl2) [23], was originally recognized as a proto-oncogenic protein. Toll-like receptors (TLRs) are innate immune sensors stimulated by specific microbial and viral components, including HCV. *In vitro* HCV infection directly induces TLR4 expression and activates human B cells to increase the production of IFN- $\beta$  and IL-6 [24]. Peripheral blood mononuclear cells from HCV-infected individuals express higher TLR4 levels compared with uninfected controls [24]. In the IKK-NF- $\kappa$ B pathway, certain activated TLRs, including TLR4, induce inhibition of kappa B kinase (IKK)-catalyzed phosphorylation of nuclear factor kappa B (NF- $\kappa$ B) p105. Nonphosphorylated NF- $\kappa$ B p105 forms a stable, inactive complex with MAP3K8. Subsequent ubiquitination and proteasome-mediated processing of NF- $\kappa$ B-p105 to NF- $\kappa$ B-p50 releases MAP3K8, which activates the MAPK/ERK kinase (MEK)-extracellular signal-regulated kinase (ERK) pathway. MEK-ERK regulates the expression of pro- and anti-inflammatory mediators that lead to the production of various cytokines and chemokines in a stimulus- and cell/receptor type-specific manner (Fig. S3, Fig. S4) [25,26]. Indeed, MAP3K8 is an important and novel therapeutic target for inflammatory diseases [27]. MAP3K8 is involved in ERK signaling activation in hepatic Kupffer and stellate cells with being stimulated by TLR4 and TLR9, leading to ERK-dependent expression of the fibrogenic genes IL-1 $\beta$  and TIMP-1. Thus, MAP3K8 expression may contribute to liver fibrosis [28].

In addition, this study provided a novel insight into MAP3K8, which is involved in resistance to HCV treatment. The results of experiments in this study demonstrated the importance of MAP3K8 in HCV production. MAP3K8 knockdown by siRNA altered extracellular, but not intracellular, HCV core antigen levels. This result suggests that MAP3K8 might be involved in the release or assembly of HCV, does not exclude the possibility that MAP3K8 participates in intracellular HCV core production because miR-17-5p influenced both supernatant and cell-lysate HCV core antigen levels along with MAP3K8 mRNA and protein levels. If MAP3K8 limited viral release/assembly alone, intracellular HCV core antigen would accumulate following siRNA transfection. Conversely, MAP3K8 overexpression did not affect HCV production, probably because enough MAP3K8 may exist in the cells. This result is generally observed in other critical host factors (e.g. hVAP-33) involved in the HCV life cycle [29]. The above description [24–26] and *in silico* analyses (Fig. S3, Fig. S4) suggest that MAP3K8 might play a role in HCV production through a regulatory pathway and network (Fig. S5); however, the exact mechanism remains unknown and requires further investigation. It is important to note that there may be differences between the HCV genotype 1b- and 2a-derived strains/replicons. The 2a-derived JFH1 infection system is highly competent compared with other genotype-derived systems and allows steady inhibition and expression analyses [30]. Notably, this *in vitro* study focused on the correlation between MAP3K8 and miR-17-5p and their impact on HCV production; there may not be significant genotypic effect on MAP3K8 and miR-17-5p. Importantly, it is difficult to determine genotype-specific differences using different infection-competent systems.

The miR-17-92 polycistron, also known as the first oncomir, encodes six or seven miRNAs, including miR-17-5p [31,32], and is frequently overexpressed in several tumors [31,33]. In contrast, overexpression of miR-17-5p also leads to tumor suppression in breast cancer [34] and HeLa cells [32]. miR-17-5p may function as both a tumor suppressor and an oncogenic activator by targeting both pro- and anti-proliferative genes and by competing with each other in different cellular contexts, which are dependent on the expression of other transcriptional regulators [35]. Known targets of the miR-17-92 cluster primarily regulate cell cycle progression, apoptosis, and transcription factors [32,35]. Physiologically, this cluster is down-regulated during aging, and hematopoietic and lung differentiation. During HIV infection, suppression of this cluster by the virus is required for efficient viral replication [36]. Our results suggest that inhibition of miR-17-5p expression may be advantageous for HCV production. Interestingly, miR-17-5p overexpression in HeLa cells decreases the expression of the low-density lipoprotein (LDL) receptor (LDLR) and consequently induces reduced intracellular lipoprotein accumulation because of the impaired internalization [32]. LDLR is one of putative HCV receptors; however, its precise role remains controversial [37-40]. LDLR also aids the optimization of HCV replication, and the expression levels are stimulated by HCV infection. Decreased LDLR and lipoprotein uptake through LDLR may adversely affect the HCV life cycle because hepatocyte lipid metabolism pathways are required for HCV.

Bioinformatics and *in vitro* experiments showed that miR-17-5p expression levels were inversely correlated with MAP3K8 in response to anti-HCV treatment. miR-17-5p repressed HCV production by inhibiting MAP3K8 expression, whereas miR-17-5p expression was influenced by MAP3K8. The results also suggested a specific interaction between miR-17-5p and MAP3K8 3'UTR, which was previously validated by the luciferase reporter assay [35]. Taken together, MAP3K8 expression following HCV infection is negatively influenced by miR-17-5p at both the translational and transcriptional levels. This molecular interaction is a potential target for novel molecular therapeutics. However, a single miRNA can regulate the expression of multiple target mRNAs by imperfect base pairing [9,10]. Conversely, the expression of a single mRNA may be regulated by several miRNAs. Numerous mRNAs and miRNAs are key regulators in complicated pathophysiological networks (Fig. S3, Fig. S4). Therefore, it is important to note that the complex interaction between MAP3K8 and miR-17-5p may not be reflective of a correlation between their expression and viral load in our patient cohort.

Abundant hepatic miR-122 expression is essential for efficient HCV replication in cultured human hepatoma cells [11]. Suppression of miR-122 leads to a marked reduction and long-lasting suppression of HCV RNA in both sera and the livers of nonhuman primates with chronic HCV infection [41]. Paradoxically, this study showed significantly lower miRNA-122 (hsa-miR-122-5p) expression levels in null/partial responders than in SVRs/relapsers, independent of other factors. This finding is in agreement with the results of a previous study, which reported markedly low baseline miR-122 levels in poor responders [21]. Moreover, no positive correlation was observed between miR-122 expression and viral load. No convincing explanation exists for these paradoxical results. Re-analysis of registered miRNA microarray data [8] identified significantly low miR-122 levels, no change in miR-675-5p levels, and low (although not significant) miR-17-5p levels in null/partial responders. Most miR-122 target genes are involved in the lipid biogenesis pathway [42], and miR-122 antagonism induces a substantial decrease in plasma lipid

levels. As described above, host lipid metabolism is vital to HCV [40], and may be related to the endogenous IFN response to HCV and IL28B SNPs [43]. However, we did not find a correlation between miR-122 expression and serum lipid levels nor identify miR-122 target genes, including lipid-related metabolic pathways, which could be considered key molecular signatures contributing to a null/partial response.

In conclusion, both global mRNA and miRNA expression profiling analyses increase our understanding of the molecular mechanisms that underlie refractory treatment responses and are even applicable to next-generation treatment. The results obtained in this study also aid the identification of novel features of known genes and target molecules for future therapeutic intervention.

## Supporting Information

**Figure S1 Hierarchical cluster analysis of mRNA expression using microarray analysis.** Changes in mRNA expression levels are presented in graduated color patches from green (least expression) to red (most abundant expression). (TIF)

**Figure S2 Hierarchical cluster analysis of miRNA expression using microarray analysis.** Changes in gene expression are presented in graduated color patches from blue (least expression) to red (most abundant expression). (TIF)

**Figure S3 Relationship between MAP3K8 (Tpl2/Cot) and related genes in underlying gene regulatory networks.** MAP3K8 (Tpl2/Cot) was integrated by Kyoto Encyclopedia of Genes and Genomes (KEGG) Pathways. MAP3K8 (Tpl2/Cot) was identified as an important node and considered to be a key regulator. (TIF)

**Figure S4 Gene networks for MAP3K8 and hsa-miR-17.** MAP3K8 and hsa-miR-17 and array-independent/literature-based text-mining were integrated into the gene regulatory network analysis (Agilent Literature Search). The interaction data were visualized and analyzed by Cytoscape. MAP3K8 and its related mRNAs were associated with the miR-17 cluster family and its related miRNAs via IRF6, STAT3, AKT1, EPHB2, TIMP1, and VEGFA. (TIF)

**Figure S5 Postulated scheme for HCV replication regulated by MAP3K8 and hsa-miR-17-5p.** IKK, inhibition of kappa B kinase; NF- $\kappa$ B, nuclear factor kappa B; MAP3K8, mitogen-activated protein kinase kinase kinase 8; MEK, MAPK/extracellular signal-regulated kinase. (TIF)

**Table S1 Comparison of baseline profiles between SVRs/relapsers and null/partial responders.** (DOC)

**Data S1 List of gene probe sets up- and down-regulated in sustained virological responders (SVR) and relapsers compared with those in null responders.** (XLS)

**Data S2 List of microRNA probe sets up- and down-regulated in sustained virological responders (SVR) and relapsers compared with those in null responders.** (XLS)

**Data S3 List of all gene probe sets up- and down-regulated in sustained virological responders (SVR) and**

## relapsers compared with those in null responders, and gene signatures in previously reported references.

(XLS)

## Acknowledgments

We thank Dr. Takaji Wakita (National Institute of Infectious Diseases) for providing the JFH1-transfected cells and Haruyo Aoyagi (National Institute

of Infectious Diseases), Rie Agata, and Yoko Yumoto (Jikei University School of Medicine) for their excellent technical support.

## Author Contributions

Conceived and designed the experiments: AT HA. Performed the experiments: AT HA K. Miyaguchi. Analyzed the data: AT K. Mogushi HA K. Miyaguchi TK TF HT. Contributed reagents/materials/analysis tools: AT KN HM TM TF. Wrote the paper: AT.

## References

- Ghany MG, Nelson DR, Strader DB, Thomas DL, Seeff LB (2011) An update on treatment of genotype 1 chronic hepatitis C virus infection: 2011 practice guideline by the American Association for the Study of Liver Diseases. *Hepatology* 54: 1433–1444.
- Kumada H, Toyota J, Okanoue T, Chayama K, Tsubouchi H, et al. (2012) Telaprevir with peginterferon and ribavirin for treatment-naive patients chronically infected with HCV of genotype 1 in Japan. *J Hepatol* 56: 78–84.
- Hayashi N, Okanoue T, Tsubouchi H, Toyota J, Chayama K, et al. (2012) Efficacy and safety of telaprevir, a new protease inhibitor, for difficult-to-treat patients with genotype 1 chronic hepatitis C. *J Viral Hepat* 19: e134–142.
- Chen L, Borozan I, Feld J, Sun J, Tannis LL, et al. (2005) Hepatic gene expression discriminates responders and nonresponders in treatment of chronic hepatitis C viral infection. *Gastroenterology* 128: 1437–1444.
- Feld JJ, Nanda S, Huang Y, Chen W, Cam M, et al. (2007) Hepatic gene expression during treatment with peginterferon and ribavirin: Identifying molecular pathways for treatment response. *Hepatology* 46: 1548–1563.
- Sarasin-Filipowicz M, Oakeley EJ, Duong FH, Christen V, Terracciano L, et al. (2008) Interferon signaling and treatment outcome in chronic hepatitis C. *Proc Natl Acad Sci USA* 105: 7034–7039.
- Honda M, Sakai A, Yamashita T, Nakamoto Y, Mizukoshi E, et al. (2010) Hepatic ISG expression is associated with genetic variation in interleukin 28B and the outcome of IFN therapy for chronic hepatitis C. *Gastroenterology* 139: 499–509.
- Murakami Y, Tanaka M, Toyoda H, Hayashi K, Kuroda M, et al. (2010) Hepatic microRNA expression is associated with the response to interferon treatment of chronic hepatitis C. *BMC Med Genomics* 3: 48.
- Lim LP, Lau NC, Garrett-Engle P, Grimson A, Schelter JM, et al. (2005) Microarray analysis shows that some microRNAs downregulate large numbers of target mRNAs. *Nature* 433: 769–773.
- Selbach M, Schwänhauser B, Thierfelder N, Fang Z, Khanin R, et al. (2008) Widespread changes in protein synthesis induced by microRNAs. *Nature* 455: 58–63.
- Jopling CL, Yi M, Lancaster AM, Lemon SM, Sarnow P (2005) Modulation of hepatitis C virus RNA abundance by a liver-specific MicroRNA. *Science* 309: 1577–1581.
- Gottwein E, Cullen BR (2008) Viral and cellular microRNAs as determinants of viral pathogenesis and immunity. *Cell Host Microbe* 3: 375–387.
- Desmet VJ, Gerber M, Hoofnagle JH, Manns M, Scheuer PJ (1994) Classification of chronic hepatitis: diagnosis, grading and staging. *Hepatology* 19: 1513–1520.
- Zhong J, Gastaminza P, Cheng G, Kapadia S, Kato T, et al. (2005) Robust hepatitis C virus infection in vitro. *Proc Natl Acad Sci USA* 102: 9294–9299.
- Wakita T, Pietschmann T, Kato T, Date T, Miyamoto M, et al. (2005) Production of infectious hepatitis C virus in tissue culture from a cloned viral genome. *Nat Med* 11: 791–796.
- Ge D, Fellay J, Thompson AJ, Simon JS, Shianna KV, et al. (2009) Genetic variation in IL28B predicts hepatitis C treatment-induced viral clearance. *Nature* 461: 399–401.
- Tanaka Y, Nishida N, Sugiyama M, Kurosaki M, Matsuura K, et al. (2009) Genome-wide association of IL28B with response to pegylated interferon-alpha and ribavirin therapy for chronic hepatitis C. *Nat Genet* 41: 1105–1109.
- Fellay J, Thompson AJ, Ge D, Gumbs CE, Urban TJ, et al. (2010) ITPA gene variants protect against anaemia in patients treated for chronic hepatitis C. *Nature* 464: 405–408.
- Urban TJ, Thompson AJ, Bradic SS, Fellay J, Schuppan D, et al. (2010) IL28B genotype is associated with differential expression of intrahepatic interferon-stimulated genes in patients with chronic hepatitis C. *Hepatology* 52: 1888–1896.
- Dill MT, Duong FHT, Vogt JE, Bibert S, Bochud PY, et al. (2011) Interferon-induced gene expression is a stronger predictor of treatment response than IL28B genotype in patients with hepatitis C. *Gastroenterology* 140: 1021–1031.
- Sarasin-Filipowicz M, Krol J, Markiewicz I, Heim MH, Filipowicz W (2009) Decreased levels of microRNA miR-122 in individuals with hepatitis C responding poorly to interferon therapy. *Nat Med* 15: 31–33.
- Miyoshi J, Higashi T, Mukai H, Ohuchi T, Kakunaga T (1991) Structure and transforming potential of the human cot oncogene encoding a putative protein kinase. *Mol Cell Biol* 11: 4088–4096.
- Patriotis C, Makris A, Bear SE, Tsichlis PN (1993) Tumor progression locus 2 (Tpl-2) encodes a protein kinase involved in the progression of rodent T-cell lymphomas and in T-cell activation. *Proc Natl Acad Sci USA* 90: 2251–2255.
- Machida K, Cheng KT, Sung VM, Levine AM, Fong S, et al. (2006) Hepatitis C virus induces toll-like receptor 4 expression, leading to enhanced production of beta interferon and interleukin-6. *J Virol* 80: 866–874.
- Banerjee A, Gerondakis S (2007) Coordinating TLR-activated signaling pathways in cells of the immune system. *Immunol Cell Biol* 85: 420–424.
- Gantke T, Sriskantharajah S, Sadowski M, Ley SC (2012) IκB kinase regulation of the TPL-2/ERK MAPK pathway. *Immunol Rev* 246: 168–182.
- George D, Salmeron A (2009) Cot/Tpl-2 protein kinase as a target for the treatment of inflammatory disease. *Curr Top Med Chem* 9: 611–622.
- Perugorria MJ, Murphy LB, Fullard N, Chakraborty JB, Vyrta D, et al. (2013) Tpl2/Cot is required for activation of ERK in liver injury and TLR induced TIMP-1 gene transcription in hepatic stellate cells. *Hepatology* 57: 1238–1249.
- Gao L, Aizaki H, He JW, Lai MM (2004) Interactions between viral nonstructural proteins and host protein hVAP-33 mediate the formation of hepatitis C virus RNA replication complex on lipid raft. *J Virol* 78: 3480–3488.
- Kato T, Matsumura T, Heller T, Saito S, Sapp RK, et al. (2007) Production of infectious hepatitis C virus of various genotypes in cell cultures. *J Virol* 81: 4405–4411.
- He L, Thomson JM, Hemann MT, Hernandez-Monge E, Mu D, et al. (2005) A microRNA polycistron as a potential human oncogene. *Nature* 435: 828–833.
- Serva A, Knapp B, Tsai YT, Claas C, Lisauskas T, et al. (2012) miR-17-5p regulates endocytic trafficking through targeting TBC1D2/Arms. *PLoS One* 7: e52555.
- Volinia S, Calin GA, Liu CG, Ambs S, Cimmino A, et al. (2006) A microRNA expression signature of human solid tumors defines cancer gene targets. *Proc Natl Acad Sci USA* 103: 2257–2261.
- Hossain A, Kuo MT, Saunders GF (2006) Mir-17-5p regulates breast cancer cell proliferation by inhibiting translation of AIB1 mRNA. *Mol Cell Biol* 26: 8191–8201.
- Cloonan N, Brown MK, Steptoe AL, Wani S, Chan WL, et al. (2008) The miR-17-5p microRNA is a key regulator of the G1/S phase cell cycle transition. *Genome Biol* 9: R127.
- Triboulet R, Mari B, Lin YL, Chable-Bessia C, Bennasser Y, et al. (2007) Suppression of microRNA-silencing pathway by HIV-1 during virus replication. *Science* 315: 1579–1582.
- Albecka A, Belouzard S, Op de Beeck A, Descamps V, Goueslain L, et al. (2012) Role of low-density lipoprotein receptor in the hepatitis C virus life cycle. *Hepatology* 55: 998–1007.
- Bassendine MF, Sheridan DA, Bridge SH, Felmlee DJ, Neely RD (2013) Lipids and HCV. *Semin Immunopathol* 35: 87–100.
- Schaefer EA, Chung RT (2013) HCV and host lipids: an intimate connection. *Semin Liver Dis* 33: 358–368.
- Syed GH, Tang H, Khan M, Hassanein T, Liu J, et al. (2014) Hepatitis C virus stimulates low-density lipoprotein receptor expression to facilitate viral propagation. *J Virol* 88: 2519–2529.
- Lanford RE, Hildebrandt-Eriksen ES, Petri A, Persson R, Lindow M, et al. (2010) Therapeutic silencing of microRNA-122 in primates with chronic hepatitis C virus infection. *Science* 327: 198–201.
- Kritzfeldt J, Rajewsky N, Braich R, Rajeev KG, Tuschl T, et al. (2005) Silencing of microRNAs in vivo with ‘antagomirs’. *Nature* 438: 685–689.
- Li JH, Lao XQ, Tillmann HL, Rowell J, Patel K, et al. (2010) Interferon-lambda genotype and low serum low-density lipoprotein cholesterol levels in patients with chronic hepatitis C infection. *Hepatology* 51: 1904–1911.

## Safety and Efficacy of Partial Splenic Embolization in Telaprevir-based Triple Therapy for Chronic Hepatitis C

Chisa Kondo<sup>1</sup>, Masanori Atsukawa<sup>1</sup>, Akihito Tsubota<sup>2</sup>, Noritomo Shimada<sup>3</sup>, Hiroshi Abe<sup>4</sup>, Norio Itokawa<sup>1</sup>, Ai Nakagawa<sup>1</sup>, Takeshi Fukuda<sup>5</sup>, Yoko Matsushita<sup>5</sup>, Katsuhisa Nakatsuka<sup>5</sup>, Chiaki Kawamoto<sup>5</sup>, Katsuhiko Iwakiri<sup>1</sup>, Yoshio Aizawa<sup>4</sup> and Choitsu Sakamoto<sup>5</sup>

### Abstract

**Objective** Pegylated-interferon/ribavirin (peg-IFN/RBV) therapy with a protease inhibitor is the standard therapy for genotype 1b chronic hepatitis C. Despite improving treatment outcomes, patients with thrombocytopenia are often difficult to treat because interferon commonly exacerbates thrombocytopenia. In this study, partial splenic embolization (PSE) was performed in patients with hypersplenism-induced thrombocytopenia to determine the effectiveness of this method as a potential treatment.

**Methods** Patients were pretreated with PSE and then received triple combination therapy. The safety and efficacy of PSE was evaluated.

**Results** Eighteen patients were analyzed, including 12 patients with the *interleukin 28B* (*IL28B*) major genotype and 12 patients with the inosine triphosphatase (*ITPA*) major genotype. The median embolization rate with PSE was 70% (range: 40-85%). PSE increased the patients' platelet counts from  $71.5 \times 10^3/\mu\text{L}$  ( $53-99 \times 10^3/\mu\text{L}$ ) to  $121.5 \times 10^3/\mu\text{L}$  ( $70-194 \times 10^3/\mu\text{L}$ ;  $p=0.0002$ ). The patients' platelet counts fluctuated above  $50 \times 10^3/\mu\text{L}$  during the treatment. Specifically, the increase in the platelet count was significantly associated with the *ITPA* major genotype compared with the minor genotype ( $p=0.0057$  at 2 weeks,  $p=0.0031$  at 3 weeks, and  $p=0.0148$  at 4 weeks). Adherence to peg-IFN- $\alpha 2b$  was sufficient ( $1.38 \mu\text{g}/\text{kg}/\text{week}$ ). The rapid viral response rate was 72.2% (13/18), the end of treatment response rate was 88.9% (16/18), and the sustained virological response (SVR) rate was 66.7% (12/18). The SVR rate for patients with the *IL28B* major genotype was 83.3% (10/12). No adverse effect due to PSE pretreatment was found in any patients. Furthermore, no patient discontinued treatment due to thrombocytopenia.

**Conclusion** PSE, in conjunction with triple combination therapy, is a useful and safe method to treat genotype 1b chronic hepatitis C patients with hypersplenism-induced thrombocytopenia.

**Key words:** partial splenic embolization, telaprevir, pegylated-interferon, ribavirin, chronic hepatitis C, thrombocytopenia

(Intern Med 54: 119-126, 2015)

(DOI: 10.2169/internalmedicine.54.3066)

### Introduction

Up to 170 million people worldwide have chronic hepati-

tis C (1), which is known to progress to liver cirrhosis, a major risk factor for the development of hepatocellular carcinoma, over a time span of several decades (2, 3). Approximately 662,000 people around the world die of hepatocellu-

<sup>1</sup>Division of Gastroenterology, Department of Internal Medicine, Nippon Medical School Chiba Hokusoh Hospital, Japan, <sup>2</sup>Core Research Facilities for Basic Science, Research Center for Medical Sciences, The Jikei University School of Medicine, Japan, <sup>3</sup>Division of Gastroenterology and Hepatology, Shinmatsudo Central General Hospital, Japan, <sup>4</sup>Division of Gastroenterology and Hepatology, Department of Internal Medicine, The Jikei University School of Medicine Katsushika Medical Center, Japan and <sup>5</sup>Division of Gastroenterology and Hepatology, Department of Internal Medicine, Nippon Medical School, Japan

Received for publication April 16, 2014; Accepted for publication May 18, 2014

Correspondence to Dr. Masanori Atsukawa, momogachi@yahoo.co.jp

lar carcinoma annually (4). Patients with advanced fibrosis should be treated with antiviral therapy as soon as possible because of the increased risk of hepatocellular carcinoma (5-7). However, the efficacy of interferon (IFN)-based treatment is known to be reduced in patients with advanced fibrosis (8). Moreover, these patients often develop thrombocytopenia, which results in insufficient IFN-based antiviral therapy and poor treatment outcomes (9-13).

Therapeutic strategies have recently been reported for the induction of antiviral therapy following partial splenic embolization (PSE) or splenectomy in patients with advanced fibrosis. Foruny et al. reported a sustained virological response (SVR) rate of 38% with pegylated-IFN/ribavirin (peg-IFN/RBV) therapy following PSE for cirrhotic patients with severe hypersplenism (14). Miyake et al. assigned patients with thrombocytopenia to groups that either received or did not receive PSE and showed that favorable treatment outcomes were associated with PSE (15). However, the outcomes of IFN-based dual combination therapy for PSE-pretreated patients were unsatisfactory.

The SVR rate of peg-IFN/RBV therapy for chronic hepatitis C patients with genotype 1b was shown to be 40-50% (9, 10), while the protease inhibitor telaprevir, in combination with peg-IFN/RBV therapy, increased the SVR rate in these patients to approximately 70-80% (16-18). However, the total dosage of this triple combination therapy is often insufficient for chronic hepatitis C patients with thrombocytopenia caused by hypersplenism. PSE pretreatment prior to triple combination therapy may be useful in improving the outcomes of these patients. However, it has yet to be determined whether a pretreatment with PSE could increase the platelet counts in chronic hepatitis C patients with thrombocytopenia caused by hypersplenism prior to the administration of triple combination therapy. Furthermore, the safety of this pretreatment prior to and throughout triple combination therapy remains unknown.

To address these issues, we conducted a prospective pilot study to investigate the efficacy and safety of triple combination therapy following PSE in chronic hepatitis C genotype 1b patients with thrombocytopenia caused by hypersplenism.

---

## Materials and Methods

---

### Study subjects

Patients with hypersplenism-induced thrombocytopenia were pretreated with PSE prior to receiving telaprevir-based triple therapy. The inclusion criteria for PSE were as follows: age between 20 and 70 years, high viral load ( $>5.0$  LIU/mL) as quantified by real-time polymerase chain reaction (PCR) for hepatitis C virus (HCV) RNA, mono-infection with genotype 1b, white blood cell count  $>1,500/\mu\text{L}$ , platelet count  $\leq 100 \times 10^3/\mu\text{L}$  to  $>50 \times 10^3/\mu\text{L}$ , and hemoglobin level  $>10$  g/dL. Hypersplenism was defined as the presence of a low platelet count ( $\leq 100 \times 10^3/\mu\text{L}$ ) and an enlarged spleen

size ( $\geq 10$  cm) as evaluated by computed tomography. Platelet-associated IgG (PAIgG), platelet-binding IgG (PBIgG), and the anti-glycoprotein IIb/IIIa antibody concentrations were evaluated, and, as a consequence, idiopathic thrombocytopenic purpura was ruled out for all patients. The exclusion criteria were as follows: other liver diseases (including autoimmune hepatitis and alcoholic hepatitis), liver cirrhosis complicated with uncontrollable ascites or/and encephalopathy, severe renal disorders, abnormal thyroid function, poorly controlled diabetes, poorly controlled hypertension, medication with Chinese herbal medicine, medical history of interstitial pneumonia, severe depression, and allergies to interferon, ribavirin, and biological preparations (e.g., vaccines).

Eighteen patients who visited the Nippon Medical School Chiba Hokusoh Hospital, Shinmatsudo General Central Hospital, and Jikei University School of Medicine Katsusika Medical Center between January 2012 and December 2012 met the inclusion criteria and agreed to receive PSE followed by telaprevir with peg-IFN/RBV triple combination therapy.

The study protocol followed the ethical guidelines established in accordance with the 2008 Declaration of Helsinki and was approved by the Ethics Committee of each institution. Written informed consent was obtained from all subjects.

### Partial splenic embolization (PSE)

PSE was performed at least one month prior to the initiation of triple therapy. A catheter was inserted through the femoral artery into the main splenic artery and 0.5 g cefazolin (CEZ) was then injected via the catheter. A microcatheter (Progreat Series, Terumo Clinical Supply, Tokyo, Japan) was selectively inserted into the inferior segmental branch of the splenic artery, and 70-80% of the spleen was embolized with gelatin sponge cubes (Gelfoam<sup>®</sup>, Pfizer, Tokyo, Japan) which were soaked in 0.5 g of CEZ.

An intravenous infusion of methylprednisolone (125 mg/day) was administered for three days after the embolization treatment to suppress excessive immune reactions. A dose of 2 g/day of CEZ was concurrently administered for the same three days to prevent splenic abscesses. The splenic infarction volume was estimated by computed tomography one week after PSE. Triple combination therapy was initiated after the patient's platelet count increased to the plateau level.

### Antiviral treatment protocol

All patients received combination therapy with peg-IFN- $\alpha 2b$  (PegIntron<sup>®</sup>, MSD, Tokyo, Japan), ribavirin (Rebetol<sup>®</sup>, MSD, Tokyo, Japan), and telaprevir (Telavic<sup>®</sup>, Mitsubishi Tanabe Pharma, Osaka, Japan) for 12 weeks, followed by 12 weeks or 36 weeks of peg-IFN- $\alpha 2b$  and ribavirin. Patients received a subcutaneous injection of peg-IFN- $\alpha 2b$  (1.5  $\mu\text{g}/\text{kg}/\text{week}$ ) and orally administered ribavirin. The dose of ribavirin was adjusted by body weight (600 mg, 800 mg, and 1,000 mg per day for  $<60$  kg, 60-80 kg, and  $>80$  kg, re-



spectively). Telaprevir (750 mg) was administered every 8 hours after meals. The dosages of each drug were reduced appropriately when a critical adverse event occurred during the treatment course. Patients were followed for 24 weeks following completion of the treatment.

### Definition of a virological response

A rapid virological response (RVR) was defined as undetectable serum HCV RNA at week 4 of the treatment. Patients who were negative for the virus at the time of treatment completion were defined as having an end of treatment response (ETR). Viral breakthrough was defined as undetectable serum HCV RNA after the treatment, but with the re-appearance of serum HCV RNA during the treatment or an increase in the HCV RNA level of  $\geq 1.2$  log IU/mL from the lowest value during the treatment period. SVR was defined as a virus-negative status 24 weeks after treatment completion. Patients who exhibited an ETR but who were also positive for the virus 24 weeks after treatment completion were considered to have relapsed. Patients whose HCV RNA levels decreased by 2 log IU/mL, but never became undetectable, were considered to have had a partial response. Patients whose HCV RNA levels decreased by at least 2 log IU/mL during IFN-based therapy were considered to have had a null response.

### Laboratory tests

Peripheral blood examinations and liver function tests were performed weekly until 12 weeks after initiation of the treatment and then monthly until 24 weeks after the completion of treatment. In the biochemical tests performed before the initiation of treatment, data were obtained from patients in the fasting state. HCV RNA levels were measured using real-time PCR (COBAS AmpliPrep, Roche Diagnostics, Tokyo, Japan). Gene mutations in the core and NS5A regions of the HCV genome were determined by the direct sequencing method. Genomic DNA was extracted from whole blood using a DNA Isolation kit on a MagNA Pure LC instrument (Roche Diagnostics, Basel, Switzerland). Single nucleotide polymorphisms (SNPs) at rs8099917, which is located in the locus adjacent to the *interleukin 28B* (*IL28B*) gene on chromosome 19, were determined by real-time PCR using TaqMan SNP Genotyping Assays on a 7,500 Fast Real-Time PCR System (Applied Biosystems, Foster City, USA). The rs8099917 genotypes were classified into 2 categories: TT (major genotype) and non-TT (minor genotype: TG or GG). SNPs at rs1127354, which is located in the locus adjacent to the inosine triphosphatase (*ITPA*) gene, were similarly determined. The rs1127354 genotypes were classified into two categories: major genotype (CC) and minor genotype (non-CC; CA or AA).

### Statistical analysis

We performed the Wilcoxon signed-rank test to analyze various factors, such as the platelet count and prothrombin time, between pre- and post-PSE states. We performed the

Mann-Whitney *U* test to analyze the change in the platelet counts during the treatment. We performed Fisher's exact test to analyze the SVR rates. All statistical analyses were performed using IBM SPSS version 17.0 (IBM Japan, Tokyo, Japan). The level of significance was set at  $p < 0.05$ .

## Results

### Background

The patient population consisted of 10 men and 8 women with a median age of 62 years (range: 40-69 years), nine of whom were treatment naïve and nine who had previously undergone treatments (five relapsers, two partial responders, and two null responders) (Table). Twelve patients had the *IL28B* major genotype TT and six patients had the *IL28B* minor genotype non-TT. Twelve patients had the *ITPA* major genotype CC and six had the *ITPA* minor genotype non-CC. Eleven patients received the treatment for 24 weeks and three patients received the treatment for 48 weeks. Four patients discontinued treatment before completing the 24-week treatment course.

### Efficacy of PSE

The median PSE rate was 70% (range: 40-85%). The median platelet count was  $71.5 \times 10^3/\mu\text{L}$  ( $53-99 \times 10^3/\mu\text{L}$ ) before PSE and increased significantly to  $121.5 \times 10^3/\mu\text{L}$  ( $70-194 \times 10^3/\mu\text{L}$ ) after PSE ( $p=0.0002$ ) (Fig. 1). Previous studies indicated that the hepatic functional reserve improved before and after PSE (14); therefore, changes in the prothrombin time activity (an indicator of hepatic reserve) before and after PSE were analyzed. The median prothrombin time was 78.7% (62.3-92.3%) before PSE and increased significantly to 83.3% (64-99.8%) with the administration of triple combination therapy ( $p=0.0166$ ).

### Changes in the platelet count during the treatment according to the ITPA genotype

Many patients maintained a platelet count of at least  $50 \times 10^3/\mu\text{L}$  during the treatment (Fig. 2). The treatment was not discontinued due to thrombocytopenia in any patients. Patients with the major *ITPA* genotype were more likely to develop RBV-induced anemia but less likely to develop thrombocytopenia (19). Therefore, changes in the platelet counts were evaluated according to the *ITPA* genotype. The platelet counts were significantly higher in patients with the *ITPA* major genotype than in those with the minor genotype ( $p=0.0057$  at 2 weeks,  $p=0.0031$  at 3 weeks, and  $p=0.0148$  at 4 weeks) (Fig. 3).

### Virological responses associated with triple combination therapy

The RVR rate was 72.2% (13/18 patients), ETR rate was 88.9% (16/18 patients), and SVR rate was 66.7% (12/18 patients). The SVR rate was 83.3% (10/12 patients) in patients with the *IL28B* genotype TT and 33.3% (2/6 patients) in

Table. Baseline Clinical Characteristics and On-Treatment Factors of the Total 18 Patients

Factors	n=18
Gender (Male/Female)	10/8
Age (year)	62 (40-69)
Body weight (kg)	58.0 (40-74)
BMI (kg/m <sup>2</sup> )	21.8 (15.1-27.4)
Prior treatment response (Naïve/relapse/partial response/null response)	9/5/2/2
White blood cell count (/μL)	3,100 (1,800-4,900)
Hemoglobin (g/dL)	13.4 (10.9-15.2)
Platelet count (× 10 <sup>3</sup> /μL)	7.2 (5.3-9.9)
AST (IU/L)	68 (36-133)
ALT (IU/L)	58 (31-142)
γ-GTP (U/L)	71 (23-267)
Albumin (g/dL)	4.0 (3.3-4.5)
Total Bilirubin (mg/dL)	0.7 (0.4-1.1)
LDL-Cholesterol (mg/dL)	84 (49-136)
UA (mg/dL)	5.7 (2.8-7.7)
Alpha-fetoprotein (ng/mL)	8.9 (2.0-707.7)
Creatinine (mg/dL)	0.66 (0.49-0.88)
Glucose (mg/dL)	98 (72-156)
HCV RNA (LogIU/mL)	6.6 (5.1-7.4)
ISDR (0-1/2</unknown)	12/5/1
Core aa70 (wild/mutant/unknown)	8/9/1
Core aa91 (wild/mutant/unknown)	10/7/1
<i>IL28B</i> genotype (rs8099917) (TT/non TT)	12/6
<i>ITPA</i> genotype (rs1127354) (CC/CA or AA)	12/6
Initiation dose of Telaprevir (mg/day)	1,750 (1,500-2,250)
Total dose of Telaprevir (mg)	126,000 (73,500-189,000)
Pegylated interferon (μg/kg/week)	1.38 (0.29-1.63)
Ribavirin (mg/kg/day)	7.43 (1.65-12.99)
Duration of treatment (24week/48week/drop out)	11/3/4

Categorical variables are given as number. Continuous variables are given as median (range).

BMI: Body mass index, AST: aspartate aminotransferase, ALT: alanine aminotransferase, γ-GTP: gamma-glutamyltransferase, LDL-cholesterol: low-density lipoprotein cholesterol, UA: urine acid, ISDR: interferon sensitivity-determining region, aa: amino acid, *IL28B*: interleukin 28B, *ITPA*: inosine triphosphatase

those with the *IL28B* genotype non-TT. The SVR rate was numerically higher in the *IL28B* genotype TT patients; however, this difference was not statistically significant ( $p=0.1073$ ) (Fig. 4). According to the prior treatment response, the SVR rates were 77.8% (7/9 patients) in treatment naïve patients, 80% (4/5 patients) in relapsers, 50% (1/2 patients) in partial responders, and 0% (0/2 patients) in null responders. Four patients relapsed, one developed viral breakthrough, and one patient had a null response.

#### Adherence of each drug

Median drug doses were sufficient at 1.38 μg/kg/week (0.29-1.63 μg/kg/week) for peg-IFN-α2b, 7.43 mg/kg/day (1.65-12.99) for RBV, and 126,000 mg (73,500-189,000) for total telaprevir.

#### Safety

All patients developed mild pyrexia and abdominal pain following PSE but recovered with symptomatic treatment

and did not develop serious complications.

Four patients discontinued triple combination therapy due to the occurrence of hepatocellular carcinoma in two patients, viral breakthrough in one patient, and acute pancreatitis in one patient. No patient discontinued the treatment due to cytopenia.

## Discussion

Patients with advanced fibrosis often have thrombocytopenia due to hypersplenism (20, 21). These patients cannot achieve favorable outcomes with antiviral IFN-based therapy because a reduction in the dose administered or discontinuation of the treatment is frequently needed due to IFN-induced thrombocytopenia (9-11). This adverse effect reduces the effectiveness of the treatment even in telaprevir-based triple therapy, which has been shown to markedly improve the SVR rate, particularly in patients with advanced fibrosis complicated by thrombocytopenia. To overcome this

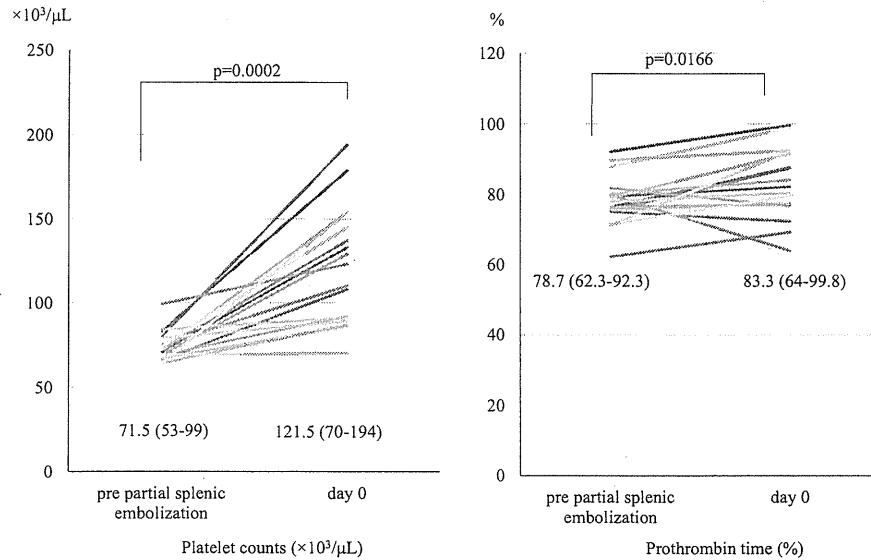


**Figure 1. Changes in the platelet counts and prothrombin times before and after partial splenic embolization. Day 0 refers to the time at which triple combination therapy was started.**

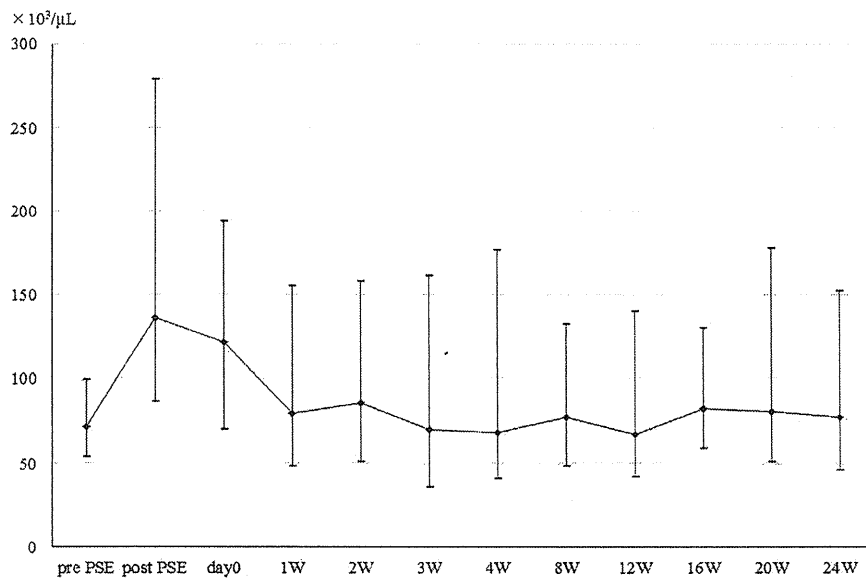


**Figure 2. Changes in the platelet counts during telaprevir/pegylated interferon/ribavirin combination therapy. Day 0 refers to the time at which triple combination therapy was started. PSE: partial splenic embolization**

therapeutic difficulty, surgical splenectomy or PSE has been performed to artificially increase blood cell counts before IFN-based therapy (14, 15, 22, 23). However, the efficacy and safety of PSE before the initiation of triple combination therapy with the protease inhibitor telaprevir has not yet been investigated.

In a previous study on triple combination therapy for treatment-naïve chronic hepatitis C patients, 231 of 1,088 (21%) patients had bridging fibrosis or compensated cirrhosis (16). These patients achieved a significantly higher SVR rate when treated with triple combination therapy (62%, 45 of 73 patients) than with peg-IFN/RBV therapy (33%, 24 of

73 patients).

Sherman et al. administered triple combination therapy to 540 treatment-naïve patients and noted that the SVR rate in patients with bridging fibrosis or compensated cirrhosis was 63% when the treatment was completed, but was only 31% when the treatment was discontinued (18). Furthermore, triple combination therapy was very effective even in patients with fibrosis; therefore, the scheduled treatment could be successfully completed. The findings of these studies indicate that triple combination therapy may be more effective than conventional peg-IFN/RBV therapy in patients with advanced fibrosis who are able to complete the treatment.

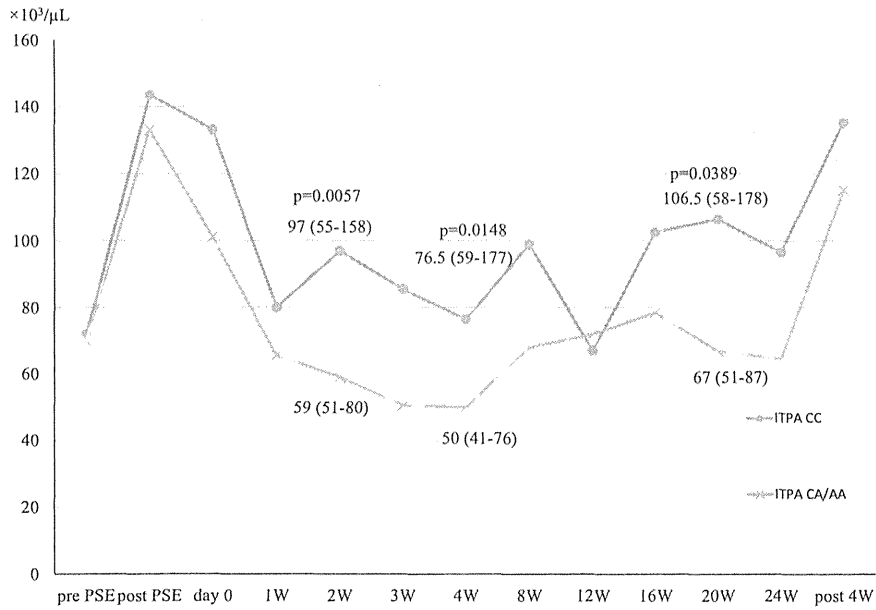


Figure 3. Comparison of the platelet counts according to the patient's ITPA genotype during triple combination therapy. Day 0 refers to the time at which triple combination therapy was started. PSE: partial splenic embolization

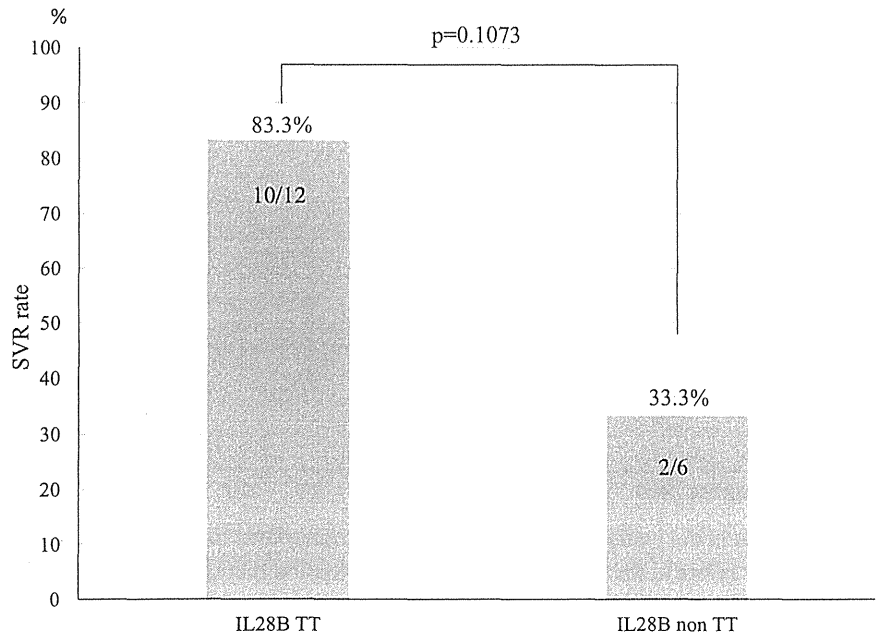


Figure 4. Comparison of the sustained virological response rates according to the patient's *IL28B* genotype.

Several studies have investigated various approaches to facilitate interferon-based treatment completion as well as treatment outcomes. Tahara et al. compared the outcomes of peg-IFN/RBV, IFN/RBV, or peg-IFN therapy in 25 patients who underwent PSE pretreatment and 23 patients who did not. Although the platelet counts during the treatment were significantly higher in the PSE group, no significant differences were observed in the SVR rate between the PSE (8%)

and non-PSE groups (7%) (22). Foruny et al. reported that the SVR rate was 38% in eight patients with advanced fibrosis who underwent PSE before peg-IFN/RBV therapy (14). Miyake et al. compared the outcomes of ten patients who underwent PSE followed by peg-IFN/RBV therapy or recombinant IFN/RBV therapy with a ten-patient historical control group that underwent peg-IFN/RBV therapy or recombinant IFN/RBV therapy without prior PSE. The